

Modeling and Investigation of Refrigeration System Performance with Two-Phase Fluid Injection in a Scroll Compressor

Rui Gu
Marquette University

Recommended Citation

Gu, Rui, "Modeling and Investigation of Refrigeration System Performance with Two-Phase Fluid Injection in a Scroll Compressor" (2016). *Master's Theses (2009 -)*. Paper 357.
http://epublications.marquette.edu/theses_open/357

MODELING AND INVESTIGATION OF
REFRIGERATION SYSTEM PERFORMANCE WITH
TWO-PHASE FLUID INJECTION IN A SCROLL
COMPRESSOR

By
Rui Gu

A Thesis Submitted to the Faculty of the
Graduate School, Marquette University,
in Partial Fulfillment of the Requirements for the
Degree of Master of Science

Milwaukee, Wisconsin

May 2016

PREFACE

MODELING AND INVESTIGATION OF REFRIGERATION SYSTEM
PERFORMANCE WITH TWO-PHASE FLUID INJECTION IN A SCROLL
COMPRESSOR

Rui Gu

Under the supervision of Professor Hyunjae Park
and Professor Anthony Bowman
Marquette University, 2016

to circulate and to have copied for non-commercial purposes, at its
discretion, the above title upon the request of individuals or institutions.

To My Parents and Friends

ABSTRACT

MODELING AND INVESTIGATION OF REFRIGERATION SYSTEM PERFORMANCE WITH TWO-PHASE FLUID INJECTION IN A SCROLL COMPRESSOR

Rui Gu
Marquette University, 2016

Vapor compression cycles are widely used in heating, refrigerating and air-conditioning. A slight performance improvement in the components of a vapor compression cycle, such as the compressor, can play a significant role in saving energy use. However, the complexity and cost of these improvements can block their application in the market. Modifying the conventional cycle configuration can offer a less complex and less costly alternative approach. Economizing is a common modification for improving the performance of the refrigeration cycle, resulting in decreasing the work required to compress the gas per unit mass. Traditionally, economizing requires multi-stage compressors, the cost of which has restrained the scope for practical implementation. Compressors with injection ports, which can be used to inject economized refrigerant during the compression process, introduce new possibilities for economization with less cost. This work focuses on computationally investigating a refrigeration system performance with two-phase fluid injection, developing a better understanding of the impact of injected refrigerant quality on a refrigeration system performance as well as evaluating the potential COP improvement that injection provides based on refrigeration system performance provided by Copeland.

ACKNOWLEDGMENTS

Rui Gu
Marquette University, 2016

I would like to express my emotions in a chronological order.

I was also so fortunate to work with Dr. Mathison, my first foreign advisor, during my time at Marquette. Thank you for guiding me through the early years of chaos and confusions, for sparking my interest in the thermal sciences, and for encouraging and supporting me to insist on my research career. I appreciate all the opportunities that you have provided me, and the time you have spent on me. After that, I was so sorry that she had to leave Marquette for her hometown due to her family issues. I understood her situation well and prayed for her family, but I faced the dilemma in my life. Graduated as MS degree or continue my Ph.D. work by myself?

I was so lucky to meet Dr. Park, my current supervisor and Dr. Bowman, my favorite professor to help me walk through the difficult situation. I decided to switch to the MS degree following their advice and recommendations at last. I appreciated their guidances and supports they had given at that time. I cannot thank you enough for all you have done when I am trapped in. Now I feel satisfied about my situation.

Dr. Park found this relevant master project for me based on my previous research, pictured the panorama of my new program and held the right research direction. Dr. Bowman expressed his interest in my work as well and supplied me

a perspective on my own results. He shared with me his knowledge and provided many useful references and friendly encouragement. I appreciate all the efforts you have made for my project.

I would also like to thank all my friends. They are wonderful people. I appreciate all the support and friendship that I have received.

Finally, I would not be where I am today without the help of my family. Thank you to my parents for your love. You have always been there to help and support me, no matter what kind of situations. Thank you for believing in me and for always supporting me to pursuing my dreams.

Table of Contents

Abstract	i
Acknowledgments	ii
List of Tables	vii
List of Figures	viii
1 Introduction	1
1.1 Background	1
1.2 Problem Statement	2
1.3 Objective	3
1.4 Literature Survey	5
2 Analysis of Refrigeration System Based on a Copeland Scroll Compressor Performance Data	9
2.1 Conventional Vapor Refrigeration Cycle	9
2.1.1 Introduction of the System	9
2.1.2 Thermodynamic Analysis of the System	11
2.1.3 Model of The System.....	13
2.1.4 Sample Calculation.....	14
2.2 Compressor Selection and Copeland Compressor Testing Cycle.....	18
2.3 Model Results	21
2.3.1 Correlation between Compressor Efficiency and Compression Pressure Ratio	21
2.3.2 Correlation between Mass Flow Rate and Evaporating Temperature.....	25

2.3.3	Performance Analysis of the Refrigeration Cycle.....	26
-------	--	----

3 Prediction of the Refrigeration System Performance with Controlled Injection Pressure **29**

3.1	Introduction to Vapor Injection Refrigeration Systems	29
3.2	Refrigeration System Injected with Isenthalpic Expansion Quality Corresponding to Injection Pressure	31
3.2.1	Thermodynamic Analysis of the System	31
3.2.2	Model of the System	34
3.2.3	Sample Calculation and Model Feasibility Analysis.....	38
3.2.4	Pre-Simulation Work.....	45
3.3	Model Results	46
3.3.1	Case Study of Minimum Compressor Efficiency Group	46
3.3.2	Case Study of Maximum Compressor Efficiency Group.....	50
3.3.3	Trend Prediction of Refrigeration System Performance with Injection	53

4 Prediction of the Refrigeration System Performance with Controlled Injection Fluid Quality **57**

4.1	Refrigeration System Injected with Controlled Injection Quality.....	58
4.1.1	Thermodynamic Analysis of the System	58
4.1.2	Model of the System	61
4.2	Model Results	64
4.2.1	Continuous Case Study of Minimum Compressor Efficiency Group.....	64
4.2.2	Sensitivity Analysis of Coefficient of Performance of the Refrigeration System with Two-Phase Fluid Injection	69

5 Summary and Conclusions	73
5.1 Summary.....	73
5.2 Conclusions.....	75

List of Tables

2.1	State Point Properties of Conventional Compression Model.....	18
3.1	State Point Properties of Model with Injection.....	44
3.2	Parametric Investigation Table	46
4.1	Sensitivity Analysis of Optimal Results of Case A1 ($T_{evap} = -10^{\circ} F T_{cond} = 100^{\circ} F$)	71
4.2	Sensitivity Analysis of Optimal Results of Case A4 ($T_{evap} = 20^{\circ} F T_{cond} = 130^{\circ} F$)	71
4.3	Sensitivity Analysis of Optimal Results of Case A6 ($T_{evap} = 40^{\circ} F T_{cond} = 150^{\circ} F$).....	71
4.4	Sensitivity Analysis of Optimal Results of Case B1 ($T_{evap} = -10^{\circ} F T_{cond} = 80^{\circ} F$).....	71

List of Figures

1.1	Vapor Injection Patterns	6
2.1	Conventional Compression Cycle and P-h Diagram.	10
2.2	T-s Diagram for an Ideal Conventional Compression Cycle [1].	12
2.3	Flow Chart for the Model of Conventional Compression Cycle.....	15
2.4	ZP44K3E-TF5 Copeland Scroll Compressor Performance Data Sheet [2].	20
2.5	ZP44K3E-TF5 R-410A Operating Map (20° F Superheat, 15° F Subcool).	21
2.6	System Diagram of Copeland Test Setup [3].	22
2.7	The Correlation of Compressor Efficiency Versus Compression Pressure Ratio.	24
2.8	The Correlation of Mass Flow Rate Versus Evaporating Temperature with 95% Confidence Interval.....	26
2.9	The Correlation of COP Versus Compression Pressure Ratio.....	28
3.1	Position and Tubing Connection for Injection Ports in the Scroll Set [4].	30
3.2	Refrigeration System Schematic Showing Hardware Components, Flow Connections and State Points.	32
3.3	P-h Diagram of the Refrigeration System Performance with Controlled Injection Pressure.	33
3.4	Flow Chart for the Model of Refrigeration Cycle with Two-Phase Flow Injection.....	39
3.5	Demonstration of Group Setup.	47
3.6	Location of the Potential Performance Improvement Group.....	48
3.7	System Performance of Potential Performance Improvement Cases.	49

3.8	Location of the None Potential Performance Improvement Group.	51
3.9	System Performance of the None Potential Performance Improvement Cases.....	52
3.10	Location of the Cross Cases Group.	54
3.11	Trend Prediction of Refrigeration System Performance with Injection.	54
3.12	System Performance of Cross Cases.....	55
4.1	Refrigeration System Schematic Showing Hardware Components, Flow Connections and State Points.	59
4.2	P-h Diagram of the Refrigeration System Performance with Controlled Injection Quality	60
4.3	Temperature Profiles at Injection Port by Different Amounts of Heat transfer.....	67
4.4	Cycle Performance Improvement with Controlled Injection Quality.....	68
4.5	Injection Quality Profile.....	70

NOMENCLATURE

Symbol	Description
COP	Coefficiency of performance, -
COP_R	Coefficiency of performance of refrigeration system, -
COP_{rev}	Coefficiency of performance of reversible refrigeration system, -
h	Specific enthalpy, Btu/lbm
$h_1...h_{10}$	Specific enthalpy at cycle state point, Btu/lbm
h_{2s}	Isentropic specific enthalpy, Btu/lbm
h_{inj}	Injection specific enthalpy, Btu/lbm
i	Index of cycle state
\dot{m}	Mass flow rate, lbm/hr
$\dot{m}_1... \dot{m}_{10}$	Mass flow rate at cycle state point, lbm/hr
\dot{m}_{inj}	Injection mass flow rate, lbm/hr
\dot{m}_{total}	Total mass flow rate, lbm/hr
P	Pressure, $psia$
$P_1...P_{10}$	Pressure at cycle state point, $psia$
P_{inj}	Injection Pressure, $psia$
P_{inlet}	Suction pressure, $psia$
P_{outlet}	Discharge pressure, $psia$
\dot{Q}	Heat transfer rate, Btu/hr
\dot{Q}_{evap}	Heat transfer in evaporator, Btu/hr
\dot{Q}_{IHx}	Heat transfer in internal heater exchanger, Btu/hr
r_p	Compression pressure ratio, -
r_{p1}	First stage compression pressure ratio, -
r_{p2}	Second stage compression pressure ratio, -
$Ratio_m$	Injection mass fraction, -

Symbol	Description
$Ratio_p$	Injection pressure ratio, -
s	Specific entropy, $Btu/lbm * R$
$s_1...s_{10}$	Specific entropy at cycle state point, $Btu/lbm * R$
s_{inj}	Injection specific entropy, $Btu/lbm * R$
T	Temperature, $^{\circ} F$
$T_1...T_{10}$	Temperature at cycle state point, $^{\circ} F$
T_{cond}	Condensing temperature, $^{\circ} F$
T_{evap}	Evaporating temperature, $^{\circ} F$
T_{inj}	Injection temperature, $^{\circ} F$
\dot{W}	Power, kW
\dot{W}_{comp}	Compressor power consumption, kW
\dot{W}_{comp1}	Compressor power consumption at 1 st stage compression, kW
\dot{W}_{comp2}	Compressor power consumption at 2 nd stage compression, kW
x	Fluid quality, -
$x_1...x_{10}$	Fluid quality at cycle state point, -
x_{inj}	Injection Fluid quality, -
ΔT_{SC}	Subcooling at outlet of condenser, $^{\circ} F$
ΔT_{SH}	Superheat at inlet of compressor, $^{\circ} F$
η	Compressor efficiency, -
$\eta_{s,1}$	Compressor efficiency at 1 st stage compression, -
$\eta_{s,2}$	Compressor efficiency at 2 nd stage compression, -
$\eta_{s,inj}$	Compressor efficiency when injecting refrigerant, -
η_s	Isentropic compressor efficiency, -

ABBREVIATIONS

comp	Compressor
cond	Condensing
evap	Evaporating
EER	Energy Efficiency Ratio
EES	Engineering Equation Solver
FT	Flash Tank
inj	Injection
IHX	Intermediate Heater Exchanger

Chapter 1

Introduction

1.1 Background

In 2005, the 111.1 million households in the United States consumed 3.1 trillion kWh of energy, accounting for 22% of the nation's total energy consumption. The use of air-conditioning equipment in 91.4 million, or 82%, of these households contributes significantly to the total energy consumption, accounting for 258.0 billion kWh of energy use annually. In addition, household refrigerators, which use the same vapor compression cycle as air-conditioning equipment under different operating conditions, consume 149.5 billion kWh of energy annually. Combining these two applications, vapor compression equipment accounts for 13% of the total residential energy use in the United States [5].

The commercial building sector, responsible for 19% of the total national energy use, also uses vapor compression based refrigeration and air-conditioning equipment, and large refrigeration systems can be found in industrial applications as well, which account for 31% of total energy use. The transportation sector, where vapor compression cycles are used for vehicle air-conditioning and refrigerated transport containers, accounts for the remaining

28% of the national energy use. Therefore, the utilization of vapor compression equipment in all sectors of the U.S. market is responsible for a significant portion of the national energy consumption [5].

1.2 Problem Statement

Vapor compression cycles are widely used in heating, refrigerating and air-conditioning. A slight performance improvement in the components of a vapor compression cycle, such as the compressor, can play a significant role in saving energy use. However, the complexity and cost of these improvements can block their application in the market. Modifying the conventional cycle configuration can offer a less complex and less costly alternative approach. Economizing is a common modification for improving the performance of the refrigeration cycle, and provides a cooling effect that decreases the work required to compress the gas per unit mass. Traditionally, economizing requires multi-stage compressors, the cost of which has restrained the scope for practical implementation. Compressors with ports, which can be used to inject economized refrigerant during the compression process, introduce new possibilities for economization with less cost.

Injecting liquid or low quality refrigerant is effective for reducing the compressor exit temperature, while injecting refrigerant vapor improves the cooling or heating capacity of the system. However, very little information is available for cycles operating with injection states between these limits of liquid and vapor injection.

Theoretical work suggests that cycle performance with two-phase refrigerant injection can provide greater improvements in COP than vapor injection. Experimental work has also shown that the performance in an economized cycle driven by multi-stage compressor can be improved by increasing the number of stages. Meanwhile, it has been proved theoretically that increasing the number of injection ports would have a similar effect.

Therefore, this work focuses on computationally investigating a refrigeration system performance with two-phase injection, developing a better understanding of the impact of injected refrigerant quality on refrigeration system performance as well as evaluating the potential COP improvement that injection provides based on compressor information provided by Copeland.

1.3 Objective

First, a scroll compressor will be selected for studying the impact of two-phase injection in this work, because scroll compressor has no poppet valves and thus has a high tolerance for liquid compared to other compressors. In addition, scroll compressor has a successful history in HVAC applications. Acceptance has been quick, creating a demand for millions of units over the past 20 years. Scroll compressors have proved their reliability in that time to be as good as or better than other technologies. Since their introduction, millions of scroll compressors have seen successful service world-wide in food and grocery refrigeration, truck transportation, marine containers, and residential and light commercial air-conditioning.

To begin with, a model of conventional vapor refrigeration cycle will be developed to analyze the system performance based on a Copeland scroll compressor performance data. In order to understand the basic cycle well, the correlations of mass flow rate vs. evaporating temperature and compressor efficiency vs. pressure ratio will be detailedly developed. In addition, model results will be compared with two-phase injection cases to investigate if two-phase injection has the potential COP improvement.

Then, a model of a refrigeration system with controlled injection pressure will be developed for directly studying the impact of two-phase injection on the refrigeration system at different operating conditions that data sheet provides. Model results will show at which conditions in the data sheet two-phase injection has the potential to improve COP. Meanwhile the results will give the best system performance numerically it can achieve at what injected mass flow rate and what injected pressure for each case that has potential COP improvement.

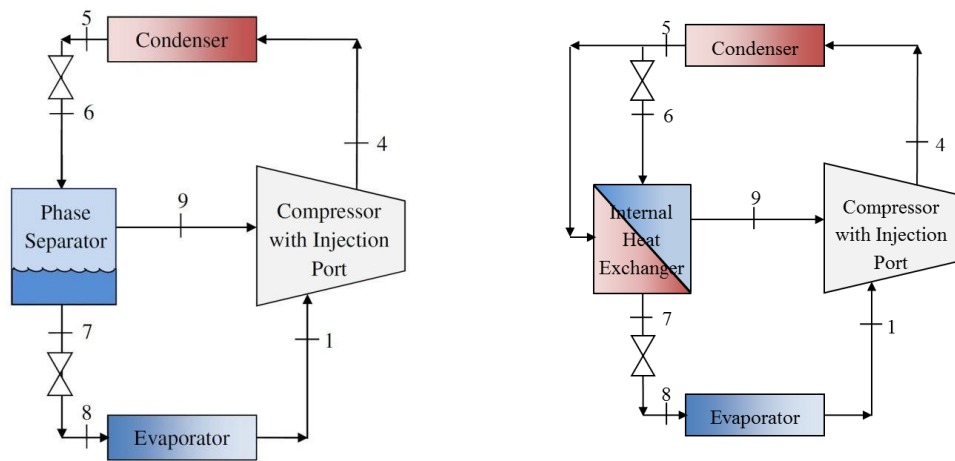
Further, a model of a refrigeration system with controlled injection fluid state will be developed in order to prevent the compressor from slugging. The model is intended to find the best system performance numerically it can reach at what injected mass flow rate, pressure and quality, taking the constraint into account. This model will give a better understanding of the effect of injected refrigerant quality on refrigeration system performance as well as evaluate the potential COP improvement that injection can reasonably provide. Besides, a differential analysis on COP of the refrigeration system with injection will be conducted at last.

1.4 Literature Survey

Experiments have shown that injecting liquid or low quality refrigerant is effective for reducing the compressor exit temperature and improving system reliability. Cho and Kim (2000) experimentally investigated the impact of liquid injection on a scroll compressor and concluded that liquid injection reduces the compressor discharge temperature [6]. Liu et al. (2008) performed experiments employing a rotary compressor with a liquid injection port, the discharge temperature dropping significantly because of the injected liquid refrigerant [7].

While liquid injection reduces the compressor discharge temperature, previous studies have demonstrated that injecting refrigerant vapor improves the cooling or heating capacity of the system. Wang et al. (2008 and 2009) conducted an experiment using vapor-injected compressor to test system performance improvement provided by both flash tank (FT) and internal heat exchanger (IHX) economization as shown in Figure 1.1. They gave similar performance improvements, increasing the capacity by up to 15% in cooling mode and 33% in heating mode as well as increasing the COP by 4% and 23% respectively, as compared to the conventional compression system with a scroll compressor [8] [9].

Vapor and liquid injection have been studied not merely experimentally but also computationally. Yamazaki et al. (2002) created a calculation program to predict the performance of the scroll compressor with liquid refrigerant injection and the modeled discharge temperature agreed very well with experimental



(a) FT vapor injection cycle schematic (b) IHX vapor injection cycle schematic
 Figure 1.1: Vapor Injection Patterns

results [10]. Winkler et al. (2008) conducted a simulation on a two-stage vapor compression system with and without a flash tank and performed experimental validation for the baseline cycle and flash tank cycle with R410A [11]. Siddharth et al. (2004) quantified the potential benefits from employing a scroll compressor with IHX vapor injection. The modeled results showed large advantages will be offered by vapor injection when the temperature lift is high; relatively smaller benefits are observed in very low temperature lift situations such as residential air conditioners [12].

Despite the many studies on cycles operating with liquid or vapor injection, very little information so far is available for cycles operating with injection states between these limits. Liu et al. (1994, 1995) studied the compression of two-phase refrigerant by developing a mathematical model and analyzed the factors causing slugging problem and the effect of compressor kinematics on slugging [13] [14]. Dutta et al. (1996) studied a two-phase refrigerant injection compression process through experiments and simulations.

Three mathematical models, droplet model, homogeneous model and slugging model were proposed. The droplet model assumed that the gaseous and liquid refrigerant exist in the control volume dividedly with different temperatures. The homogeneous model assumed that each phase of the two-phase refrigerant has the same temperature at any time instead. The slugging model assumed that the liquid and vapor refrigerant have the same temperature and the gas is always saturated vapor during the compression process. They found the homogenous model had a good agreement with the experimental results.

Theoretical work suggests that cycle performance with two-phase refrigerant injection can provide greater improvements in COP than vapor injection. Mathison et al. (2014) developed a model of an economized cycle with three injection ports compressor. The model predicts injecting saturated vapor will provide a 12% improvement in COP, which is approximately 67% of the maximum benefit provided by economizing with continuous injection of two-phase refrigerant, for an air-conditioner using R-410A with an evaporating temperature of 5°C and a condensing temperature of 40°C [15].

In addition, experimental work has showed that increasing the number of stages in an economized cycle with a multi-stage compressor improves the cycle performance and theoretical work suggests that increasing the number of injection ports would have a similar effect. Mathison et al. (2011) stimulated a vapor compression cycle with multi-port injection and flash-tank economization. The modeled results indicated the addition of the injection ports can improve COP, approaching the limit when continuously injected refrigerant kept a saturated vapor state in the compression [16].

Therefore, there is a need for further work investigating the performance of cycles with two-phase economized refrigerant injection through multiple injection ports. However, continuously injecting refrigerant is not only beyond the capabilities of current compressors, but also requires the development of equipment to continuously supply refrigerant to the compressor at the desired pressure and quality. In addition, injecting a two-phase mixture introduces the possibility for damage to the compressor if the evaporation process is not well-understood.

The current study demonstrates that injecting two-phase mixture using a finite number of injection ports provides a practical means for approaching the limiting cycle performance. Therefore, a model of a refrigeration system with one injection will be developed for investigating a refrigeration system performance with two-phase injection, developing a better understanding of the impact of injected refrigerant quality on refrigeration system performance as well as evaluating the potential COP improvement that injection provides based on compressor information provided by Copeland.

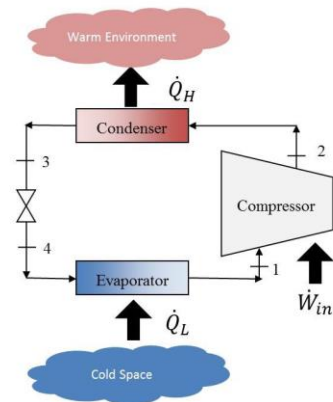
Chapter 2

Analysis of Refrigeration System Based on a Copeland Scroll Compressor Performance Data

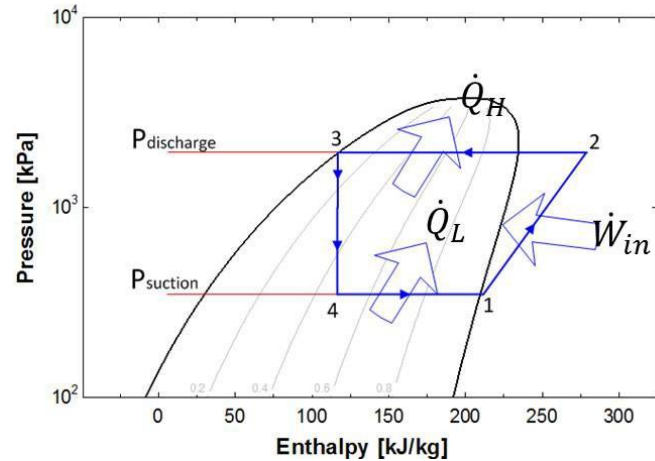
2.1 Conventional Vapor Refrigeration Cycle

2.1.1 Introduction of the System

Vapor compression cycles are widely used in heating, refrigerating and air-conditioning. Refrigeration systems use a circulating liquid refrigerant as the medium which absorbs and removes heat from the space to be cooled and subsequently rejects that heat elsewhere. Figure 2.1 depicts a typical, single-stage vapor-compression system. All such systems have four components: a compressor, a condenser, a thermal expansion valve (also called a throttling valve or metering device), and an evaporator. Circulating refrigerant enters the compressor in a thermodynamic state as a saturated vapor or slightly superheated and is compressed to a higher pressure, resulting in a higher temperature as well. The hot, compressed vapor is then in the thermodynamic state known as a superheated vapor and is at a temperature and pressure in which it can be condensed with either cooling water or cooling air. The hot vapor is routed through a condenser where it is cooled and condensed a liquid by



(a) Conventional Compression Cycle



(b) P-h Diagram

Figure 2.1: Conventional Compression Cycle and P-h Diagram.

flowing through a coil or tubes with cool water or cool air flowing across the coil or tubes. This is where the circulating refrigerant rejects heat from the system and the rejected heat is carried away by either the water or the air (whichever may be the case) [1].

The condensed liquid refrigerant, in the thermodynamic state known as a saturated liquid, is next routed through an expansion valve where it undergoes an abrupt reduction in pressure and reduction in temperature. That pressure reduction results in the adiabatic flash evaporation of a part of the liquid refrigerant. The auto-refrigeration effect of the adiabatic flash evaporation lowers the temperature of the liquid and vapor refrigerant mixture to where it is colder than the temperature of the enclosed space to be refrigerated [1].

The cold mixture is then routed through the coil or tubes in the evaporator. A fan circulates the warm air in the enclosed space across the coil or tubes carrying the cold refrigerant liquid and vapor mixture. That warm air evaporates the liquid part of the cold refrigerant mixture. At the same time, the

circulating air is cooled and thus lowers the temperature of the enclosed space to the desired temperature. The evaporator is where the circulating refrigerant absorbs and removes heat which is subsequently rejected in the condenser and transferred elsewhere by the water or air used in the condenser [1].

To complete the refrigeration cycle, the refrigerant vapor from the evaporator is again a saturated vapor and is routed back into the compressor [1].

2.1.2 Thermodynamic Analysis of the System

The thermodynamics of an ideal vapor compression cycle can be analyzed on a temperature versus entropy diagram, as depicted in Figure 2.2. At state 1 in the diagram, the circulating refrigerant enters the compressor as a saturated vapor. From state 1 to state 2, the vapor is isentropically compressed (i.e., compressed at constant entropy) and exits the compressor as a superheated vapor [1].

From state 2 to state 3, the vapor travels through part of the condenser which removes the superheat by cooling the vapor. Between state 3 and state 4, the vapor travels through the remainder of the condenser and is condensed into a saturated liquid. The condensation process occurs at essentially constant pressure [1].

Between states 4 and 5, the saturated liquid refrigerant passes through the expansion valve and undergoes an abrupt decrease of pressure. The process results in a rapid adiabatic evaporation and auto-refrigeration of a portion of the liquid (typically, less than half of the liquid flashes). The rapid adiabatic

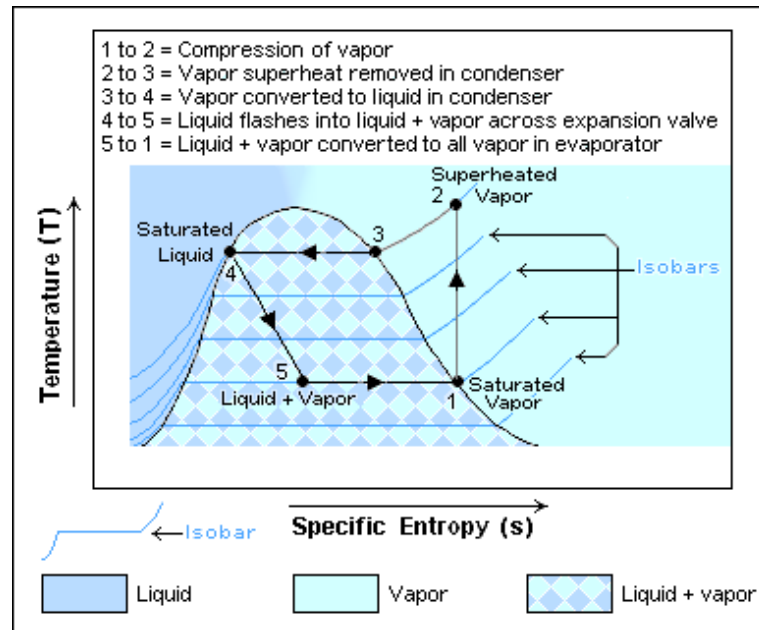


Figure 2.2: T-s Diagram for an Ideal Conventional Compression Cycle [1].

evaporation process is isenthalpic (i.e., occurs at constant enthalpy) [1].

Between states 5 and 1, the cold and partially vaporized refrigerant travels through the coil or tubes in the evaporator where it is totally vaporized by warm air (from the space being refrigerated) that a fan circulates across the coil or tubes in the evaporator. The evaporator operates at essentially constant pressure and boils off all available liquid thereafter adding 4-8 degrees of superheat to the refrigerant as a safeguard for the compressor as it cannot compress an incompressible fluid. The resulting refrigerant vapor returns to the compressor inlet at state 1 to complete the thermodynamic cycle [1].

It should be noted that the above discussion is based on the ideal vapor-compression refrigeration cycle which does not take into account real world items like frictional pressure drop in the system, internal irreversibility during the compression, or non-ideal gas behavior [1].

2.1.3 Model of the System

A model has been developed to predict its performance over the range of anticipated operating conditions. The model is intended for use with R-410A as the working fluid and will be capable of testing a variety of different compressors. The model should be easily adaptable to serve as a tool for evaluating the impact of compressor selection on system performance.

To accomplish this goal, the model uses manufacturer-supplied data to characterize the compressor performance. This data is typically provided over a range of condensing and evaporating temperatures with a specified superheat at the compressor inlet and subcooling at the condenser exit. For a compressor without injection ports, manufacturers may report the expected cooling capacity, power consumption, current draw, mass flow rate, EER and isentropic efficiency of the compressor under each condition.

Using the isentropic compressor efficiency and an adiabatic process to model the conventional compression cycle simplifies the model considerably. In addition, the following assumptions are proposed:

1. Steady-state, steady flow conditions.
2. One-dimensional flow.
3. The compressor can be modeled using an isentropic efficiency.
4. The pressure drop through pipes is negligible.
5. Compared to the heat transfer between the condenser and the heat sink, the heat transfer between the pipes and the ambient is negligible.
6. The throttling devices are isenthalpic, with no work or heat transfer.
7. Kinetic and potential energy changes are small relative to changes in

enthalpy and can be disregarded.

The conventional refrigeration system model was implemented using Engineering Equation Solver (Klein, 2009). It requires the user to specify the condensing and evaporating temperatures, degree of superheat at the compressor inlet and subcooling at the condenser outlet, compressor power input, mass flow rate and isentropic efficiency. The compressor manufacturer typically provides all of these parameters on the performance sheet. Making the assumptions mentioned above, the model then will calculate the thermodynamic properties at each state, the mass flow rate through each line in the model, and heat transfer rate in the condenser.

To make reader have a clear picture over modeling the conventional compression cycle, a flow chart is provided in Figure 2.3.

2.1.4 Sample Calculation

A very important condition, where the Copeland compressor can achieve the highest efficiency, was chosen for doing a sample hand calculation, which was intended to make sure there are no errors in the model codes by comparison between hand calculations results and simulation output. Meanwhile, this hand calculated process that follows shows the modeling procedure literally. See Figure 2.1.

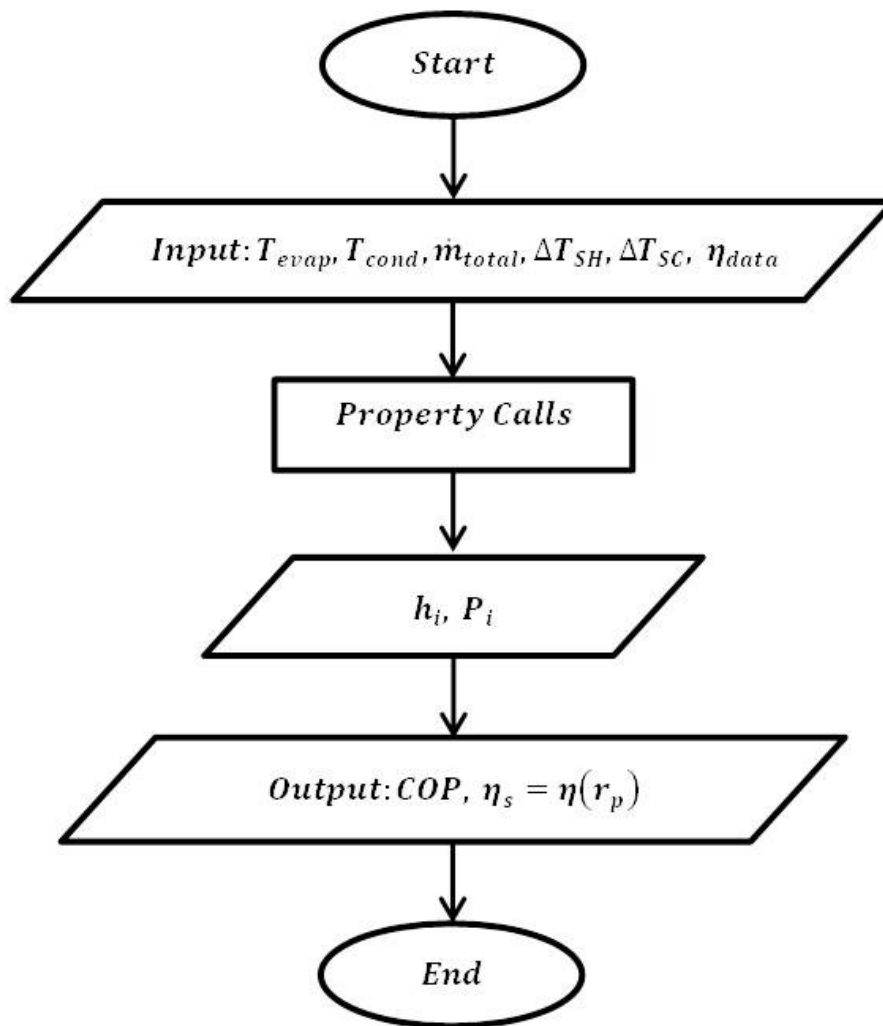


Figure 2.3: Flow Chart for the Model of Conventional Compression Cycle.

1. Operating Conditions (From Copeland Scroll Compressor Performance Data Sheet [2]):

$$T_{evap} = 45^{\circ} F, T_{cond} = 110^{\circ} F, \eta = 73.6\%, \dot{m} = 670 \text{ lbm/hr}, \Delta T_{SH} = 20^{\circ} F,$$

$$\Delta T_{SC} = 15^{\circ} F$$

2. Compressor Inlet:

$$T_1 = T_{evap} + \Delta T_{SH} = 45 + 20 = 65^{\circ} F$$

$$P_1 = \text{Pressure}(R410A, T_{evap} = 45^{\circ} F, x = 1) = 144.8 \text{ psia}$$

$$h_1 = \text{Enthalpy}(R410A, P_1 = 144.8 \text{ psia}, T_1 = 65^{\circ} F) = 187.4 \text{ Btu/lbm}$$

$$s_1 = \text{Entropy}(R410A, P_1 = 144.8 \text{ psia}, T_1 = 65^{\circ} F) = 0.44 \text{ Btu/lbm} * R$$

3. Compressor Efficiency Relation:

$$\eta_s = \frac{h_{2s} - h_1}{h_2 - h_1} = 0.736 = \frac{h_{2s} - 187.4 \text{ Btu/lbm}}{h_2 - 187.4 \text{ Btu/lbm}}$$

4. Compressor Outlet or Condenser Inlet:

$$P_2 = \text{Pressure}(R410A, T_{\text{cond}} = 110^\circ F, x = 0) = 381.1 \text{ psia}$$

$$h_{2s} = \text{Enthalpy}(R410A, P_2 = 381.1 \text{ psia}, s_{2s} = s_1)$$

$$= 199.8 \text{ Btu/lbm}$$

$$h_2 = \frac{h_{2s} - h_1}{\eta} + h_1 = \frac{199.8 - 187.4}{0.736} + 187.4 = 204.3 \text{ Btu/lbm}$$

$$T_2 = \text{Temperature}(R410A, P_2 = 381.1 \text{ psia}, h_2 = 204.25 \text{ Btu/lbm}) = 173.4^\circ F$$

$$s_2 = \text{Entropy}(R410A, P_2 = 381.1 \text{ psia}, T_2 = 173.4^\circ F) = 0.4467 \text{ Btu/lbm} * R$$

5. Condenser Outlet or Expansion Valve Inlet:

$$T_3 = T_{\text{cond}} - \Delta T_{\text{SC}} = 110 - 15 = 95^\circ F$$

$$P_3 = P_2 = 381.1 \text{ psia}$$

$$h_3 = \text{Enthalpy}(R410A, P_3 = 381.1 \text{ psia}, T_3 = 95^\circ F) = 110.4 \text{ Btu/lbm}$$

$$s_3 = \text{Entropy}(R410A, P_3 = 381.1 \text{ psia}, T_3 = 95^\circ F) = 0.2841 \text{ Btu/lbm} * R$$

6. Expansion Valve Outlet or Evaporator Inlet:

$$h_4 = h_3 = 110.4 \text{ Btu/lbm}$$

$$P_4 = P_1 = 144.8 \text{ psia}$$

$$T_4 = \text{Temperature}(R410A, P_4 = 144.8 \text{ psia}, h_4 = 110.4 \text{ Btu/lbm}) = 44.8^\circ F$$

$$s_4 = \text{Entropy}(R410A, P_4 = 144.8 \text{ psia}, T_4 = 44.8^\circ F) = 0.2872 \text{ Btu/lbm} * R$$

Table 2.1: State Point Properties of Conventional Compression Model.

State Pt No.(i)	h_i (Btu/lbm)	P_i (Psia)	s_i (Btu/lbm * R)	T_i (° F)	x_i (-)
1	187.4	144.8	0.4397	65	SHV
2	204	381.1	0.4467	172.4	SHV
3	110.4	381.1	0.2841	95	CL
4	110.4	144.8	0.2872	44.85	SLVM

7. Calculations for overall system:

$$\dot{Q}_{evap} = \dot{m} \times (h_1 - h_4) = 670 \text{ lbm/hr} \times (187.4 - 110.4) \text{ Btu/lbm} = 51590 \text{ Btu/hr}$$

$$\begin{aligned} \dot{W}_{comp} &= \dot{m} \times (h_2 - h_1) = 670 \text{ lbm/hr} \times (204.3 - 187.4) \text{ Btu/lbm} = 11323 \text{ Btu/hr} \\ &= 3318 \text{ W} \end{aligned}$$

$$COP = \frac{\dot{Q}_{evap}}{\dot{W}_{comp}} = \frac{51590}{11323} = 4.556$$

The EES program calculation results are summarized in the Table 2.1, convenient to look up and compared with hand calculation.

Due to the inevitable errors caused hand calculation, the COP of 4.556 deviate slightly from the COP of 4.677 derived by running the model in the EES program. The COP value of 4.677 will be used to prove the feasibility of the model of refrigeration system with injection in the coming Chapter 3.

2.2 Compressor Selection and Copeland Compressor Testing Cycle

In order to investigate the impact of refrigerant injection on compressor, a compressor which the injection can be apply to should be selected. As the problem statement explains, a scroll compressor has the high tolerance of liquid

since it has no poppet valves and piston inside. So scroll compressor is appropriate for this application. In addition, scroll compressors still have many other remarkable advantages that we would like to choose it for:

1. Worldwide successful history in HVAC application.
2. Proven high reliability and lower noise level due to the symmetric geometry and continuous compression without pulsation.
3. Low friction and high efficiency therefor because of non-compliant designs that no contact between the scrolls.
4. Precise machining permits sealing vane flanks with a thin film of oil.

A type of scroll compressor with the model No. ZP44K3E-TF5 has been selected from Copeland and its testing data sheet shown below in Figure 2.4 will be the basis to calculate all the desired results.

The calorimeter testing was done in Emersons A2L Research calorimeter lab test facility located in Sidney, Ohio. An R-410A Copeland Scroll ZP44K3E-TF5 was tested for an air-conditioning application. All compressor tests are performed at a refrigerants dew point temperature for suction and discharge pressure conditions. The R-410A operating envelope for the test compressor is shown in Figure 2.5. The x and y axes show dew point temperatures. There are no test points beyond 45°F evaporating temperature and curves are extrapolated to 55°F. The compressor envelope does not show performance below 80°F condensing [17].

RATING CONDITIONS
 20 °F Superheat
 15 °F Subcooling
 95 °F Ambient Air Over

AIR CONDITIONING

ZP44K3E-TF5
 HFC-410A
 COPELAND SCROLL®
 TF5 200/230-3-60

60 Hz Operation

Evaporating Temperature °F (Sat. Dew Pt Pressure, psig)

-10(36) 0(48) 10(62) 20(78) 30(97) 40(118) 45(130) 50(142) 55(155)

Condensing Temperature °F (Sat. Dew Pt Pressure, psig)															
	150 (611)	140 (540)	130 (475)	120 (417)	110 (364)	100 (316)	90 (273)	80 (235)							
C									33100	36900	40900	45100			
P									5700	5600	5550	5500			
A									16	15.9	15.7	15.5			
M									575	635	700	765			
E									5.8	6.6	7.3	8.2			
%									58.4	61.4	64.1	66.4			
C									29400	36700	40700	44900	49300		
P									5050	4920	4870	4810	4770		
A									14.4	14.1	14	13.8	13.7		
M									475	585	645	705	770		
E									5.8	7.5	8.4	9.3	10.3		
%									57	63.4	66	68.2	70		
C									25600	32500	40200	44300	48800	53500	
P									4460	4360	4270	4220	4180	4150	
A									12.9	12.7	12.5	12.4	12.3	12.2	
M									390	489	595	655	715	780	
E									5.8	7.5	9.4	10.5	11.7	12.9	
%									55.2	62.3	67.7	69.8	71.4	72.5	
C									22000	28400	35600	43500	47900	52500	57500
P									3950	3870	3790	3710	3680	3650	3620
A									11.7	11.5	11.4	11.2	11.1	11	11
M									318	405	500	605	660	725	785
E									5.6	7.4	9.4	11.7	13	14.4	15.9
%									52.9	60.8	66.8	71.1	72.5	73.3	73.6
C		18500	24500	31000	38400	46700	51500	56000	61500						
P		3500	3430	3360	3300	3240	3220	3190	3170						
A		10.7	10.5	10.4	10.3	10.1	10.1	10	9.9						
M		255	333	417	510	615	670	730	795						
E		5.3	7.1	9.2	11.6	14.4	16	17.6	19.4						
%		50.2	58.8	65.5	70.3	73	73.6	73.5	72.6						
C	15200	20700	26700	33500	41100	49800	54500	60000	65500						
P	3090	3040	2990	2940	2880	2840	2820	2800	2780						
A	9.8	9.7	9.6	9.5	9.4	9.3	9.2	9.2	9.1						
M	202	271	345	426	515	620	675	735	800						
E	4.9	6.8	8.9	11.4	14.2	17.6	19.4	21.4	23.5						
%	46.9	56.4	63.7	69	72.3	73.2	72.7	71.3	69.2						
C	17200	22700	28800	35700	43600	52500	58000	63000	69000						
P	2690	2650	2610	2560	2520	2480	2460	2450	2430						
A	8.9	8.9	8.8	8.7	8.6	8.5	8.5	8.5	8.4						
M	217	282	353	432	520	625	680	740	805						
E	6.4	8.6	11	13.9	17.3	21.2	23.5	25.8	28.4						
%	53.3	61.4	67.3	71	72.5	71.1	69.3	66.5	62.7						
C	19000	24400	30600	37700	45900	55500	61000	66500	72500						
P	2340	2300	2270	2230	2190	2160	2140	2130	2110						
A	8.2	8.2	8.1	8.1	8	7.9	7.9	7.9	7.8						
M	227	289	358	435	525	625	685	745	810						
E	8.1	10.6	13.5	16.9	20.9	25.7	28.4	31.3	34.4						
%	58.5	65.1	69.4	71.4	70.7	66.6	63.1	58.5	52.5						

Nominal Performance Values (±5%) based on 72 hours run-in. Subject to change without notice. Current @ 230 V

C-Capacity(Btu/hr), P-Power(Watts), A-Current(Amps), M-Mass Flow(lbs/hr), E-EER(Btu/Watt-hr), % Isentropic Efficiency(%)



Figure 2.4: ZP44K3E-TF5 Copeland Scroll Compressor Performance Data Sheet [2].

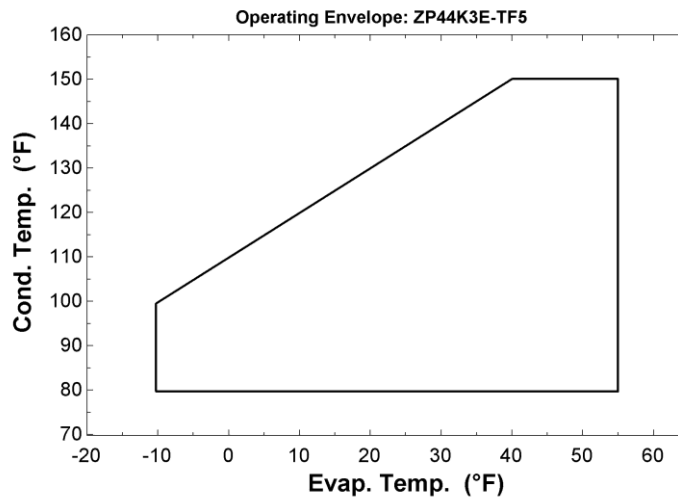


Figure 2.5: ZP44K3E-TF5 R-410A Operating Map (20°F Superheat, 15°F Subcool).

The testing load stand, shown in Figure 2.6, was intended to test compressors that operate at two different pressures. The closed loop of the test stand essentially operates using the same principle as the conventional compression cycle that supplies refrigerant to the compressor suction state.

2.3 Model Results

2.3.1 Correlation between Compressor Efficiency and Compression Pressure Ratio

Compression pressure ratio, an important parameter in compressor design and selection, is often denoted as r_p . It is defined as the ratio of the absolute discharge pressure to the absolute suction pressure in a compression process, expressed in Equation 2.3.1.

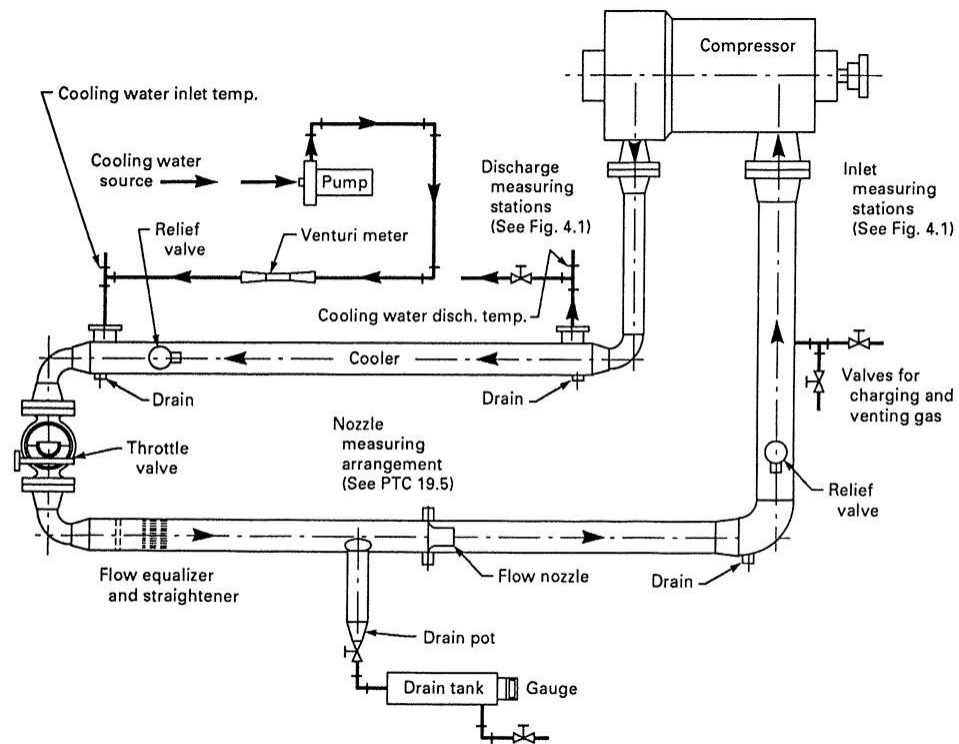


Figure 2.6: System Diagram of Copeland Test Setup [3].

$$r_p \equiv \frac{P_{outlet}}{P_{inlet}}; \quad (2.3.1)$$

In addition, r_{p1} represents the first stage compression ratio in a refrigerant-injected compressor; r_{p2} represents the second stage compression ratio in a refrigerant-injected compressor. They are expressed in the following equations 2.3.2 and 2.3.3, where P_1 represents inlet pressure; P_2 represents outlet pressure.

$$r_{p1} \equiv \frac{P_{inj}}{P_1}; \quad (2.3.2)$$

$$r_{p2} \equiv \frac{P_2}{P_{inj}}; \quad (2.3.3)$$

Compression ratio and volumetric efficiency are closely related terms. It is necessary to discuss volumetric efficiency first to understand the significance of compression ratio and its influence on the overall operation of a refrigeration system. Volumetric efficiency is a ratio of the amount of refrigerant that a compressor will theoretically compress, to what it actually compresses. In a reciprocating compressor, the piston reaches top dead center, at the completion of the discharge stroke, there is a small amount of gas that must expand before the suction reed opens which starts the suction stroke. This decreases the amount of gas that is able to enter the cylinder during the suction stroke. If the discharge pressure increases, the gas left at the top of the cylinder is denser and so it will fill up more of the cylinder upon re-expansion. The result is a smaller amount of refrigerant that is able to be compressed, resulting in a decrease in the volumetric efficiency of the compressor. If the suction pressure changes, the volumetric efficiency will change as well, and therefore the efficiency of the compressor

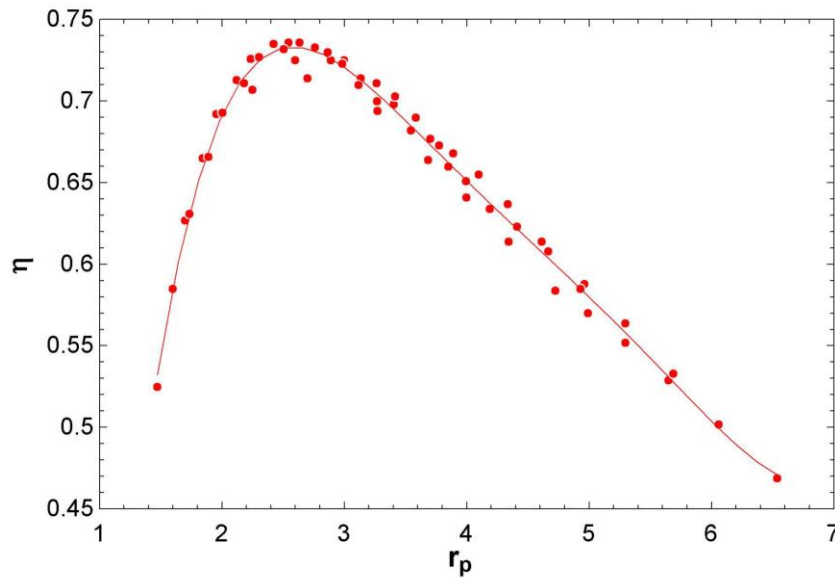


Figure 2.7: The Correlation of Compressor Efficiency Versus Compression Pressure Ratio.

changes. That's where the term compression ratio comes in. In this work, that how the compression pressure ratio affects compressor efficiency is developed in Figure 2.7 based on the manufacturer's data. There is also leakage that decreases the volumetric efficiency.

It is obviously indicated compressor efficiency can be expressed as a function of the compression ratio across the compressor. A higher discharge pressure from a dirty condenser or a lower suction pressure caused by low pressure refrigerant across the evaporator, for example, will greatly reduce system performance and compressor efficiency.

In order to simulate refrigeration system with injection, a curve fit (shown in Equation 2.3.4) is made to quantify the relationship between the compressor efficiency and compression ratio in order to interpolate the compressor efficiencies at different stages in the compression process.

$$\eta = -1.46089 + 2.65662 \times r_p - 1.2226 \times r_p^2 + 0.269856 \times r_p^3 - 0.0293404 \times r_p^4 + 0.001257 \times r_p^5 \quad (2.3.4)$$

where, $r^2 = 99.01\%$.

2.3.2 Correlation between Mass Flow Rate and Evaporating Temperature

If the flow rate of the working fluid in the refrigeration system passing through the evaporator coil is reduced without changing condenser conditions, the evaporating pressure and temperature will decrease. Based on the provided data, the correlation of mass flow rate versus evaporating temperature has been found and shown in Figure 2.8.

This plot confirms the expectations that the refrigerant mass flow rate decreases as evaporating temperature decrease. This is mainly due to the increased specific volume of the refrigerant and reduced volumetric efficiency of the compressor. Likewise, the compressor efficiency, a curve fit (shown in Equation 2.3.5) is made to quantify the relationship between mass flow rate and evaporating temperature.

$$\dot{m} = 272.633 + 5.89601 \times T_{evap} + 0.0626164 \times T_{evap}^2 \quad (lbm/hr) \quad (2.3.5)$$

where, $r^2 = 99.23\%$; \dot{m} is the mass flow rate going through all the conventional compression cycle; T_{evap} is the evaporating temperature with the unit of ° F.

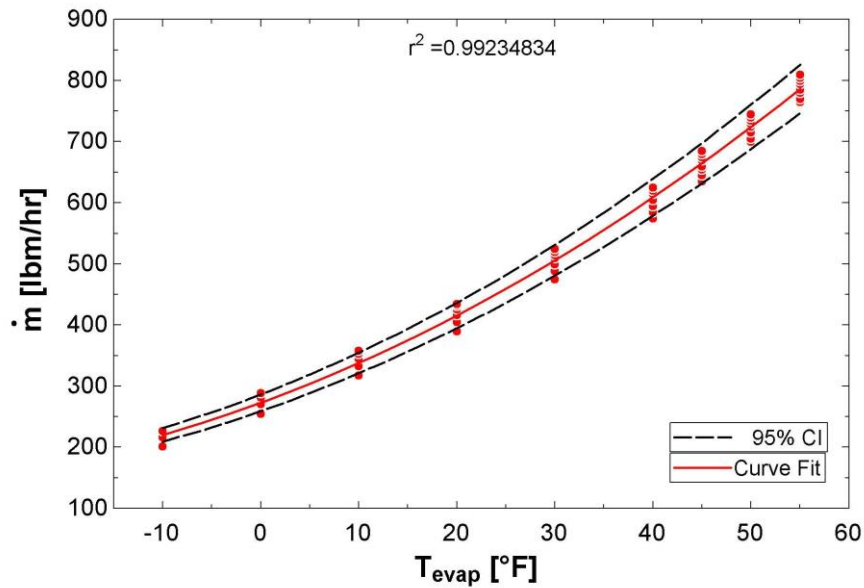


Figure 2.8: The Correlation of Mass Flow Rate Versus Evaporating Temperature with 95% Confidence Interval.

2.3.3 Performance Analysis of the Refrigeration Cycle

It is highly anticipated that improvement, if any, due to the injection can be realized in the system. So how much room does the real system still have to be improved? The upper performance limit of the refrigeration cycle will be a reference for people to look up.

The Carnot cycle is a theoretical thermodynamic cycle proposed by Nicolas Leonard Sadi Carnot in 1824 and expanded upon by others in the 1830's and 1840's. The Carnot cycle is a totally reversible cycle that consists of two reversible isothermal and two isentropic processes. It proves the maximum thermal efficiency for given temperature limits, and it serves as a standard against which actual power cycles can be compared.

Since it is a reversible cycle, all four processes that comprise the Carnot cycle can be reversed. Reversing the cycle does also reverse the directions of any heat and work interactions. The result is a cycle that operates in the counter-clockwise direction on a T-s diagram. It provides an upper limit on the Coefficient of Performance of a refrigeration system in creating a temperature difference by the application of work to the system. Meanwhile it offers the upper performance limit of the refrigeration cycle for given temperature limits. The coefficients of performance of Carnot refrigeration system are expressed in terms of temperature as:

$$COP_{rev} = \left(\frac{T_{cond}}{T_{evap}} - 1 \right)^{-1} \quad (T[=] \text{ Absolute}) \quad (2.3.6)$$

It is a theoretical system but not an actual thermodynamic cycle, since the idealizations and simplifications commonly employed in the analysis of power cycles can be summarized as follows:

1. The cycle does not involve any friction. Therefore, the working fluid does not experience any pressure drop as it flows in pipes or devices such as heat exchangers.
2. All expansion and compression processes take place in a quasi-equilibrium manner.
3. The pipes connecting the various components of a system are well insulated, and heat transfer through them is negligible.

Comparing the actual system performance the data sheet provides with that of Carnot refrigeration system, the difference between ideal and actual COPs

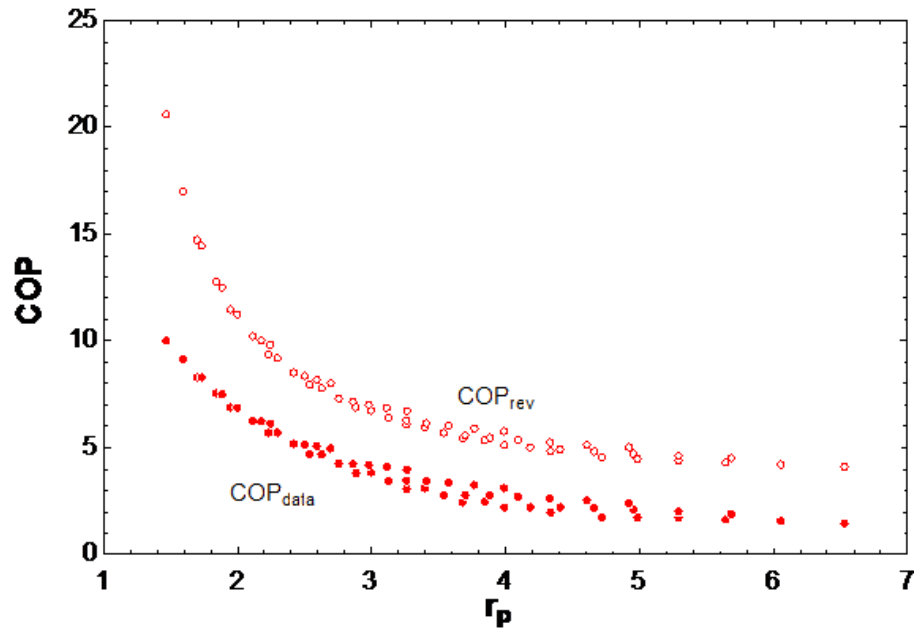


Figure 2.9: The Correlation of COP Versus Compression Pressure Ratio.

illustrates the potential for improvement. That how much room the real system still have to be improved have been displayed in the Figure 2.9.

Chapter 3

Prediction of the Refrigeration System Performance with Controlled Injection Pressure

3.1 Introduction to Vapor Injection Refrigeration Systems

The vapor injected (VI) scroll compressor makes use of an economizer within the vapor compression cycle. This cycle offers the advantages of more cooling capacity and a better COP than with a conventional cycle. Both the capacity and the COP improvement are proportional to the temperature rise. Thermodynamically the VI technology offers significant advantages in applications where temperature rise is high (e.g. water heating, space heating and refrigeration), and relatively smaller benefits in applications such as residential air conditioner where efficiency standards are based on tests conducted at very low temperature rise conditions. This could explain why VI technology is more widely known and used in residential applications in Europe and Asia, compared to the U.S. where the residential market is focused almost exclusively on air conditioning applications.



(a) Position of the Injection Ports
in the Scroll Set

(b) Internal Tubing Connecting the
Injection Inlet with the Scroll Set

Figure 3.1: Position and Tubing Connection for Injection Ports in the Scroll Set [4].

It is usually possible to specify a smaller displacement compressor for a given cooling load using VI technology. Additionally the cooling provided by the interstage injection allows the compressor to operate over a similar envelope to a conventional liquid injected model, and so the vapor-injected scroll can operate at all the normal low temperature application conditions. Therefore, the vapor injected scroll compressor has been designed and produced by Copeland. The scroll injection port location is shown schematically in Figure 3.1 .

3.2 Refrigeration System Injected with Isenthalpic Expansion Quality Corresponding to Injection Pressure

To simply investigate the effect of injection on the conventional refrigeration system, after the refrigerant comes out of condenser, it passes through an expansion valve used to control the injection pressure, then it is directly injected to injection ports on the compressor. The refrigeration system is schematically shown in Figure 3.2.

3.2.1 Thermodynamic Analysis of the System

The thermodynamics of an ideal refrigeration system injected with controlled injection pressure can be analyzed on a pressure versus enthalpy diagram as depicted in Figure 3.3. At state 1 in the diagram, the circulating refrigerant enters the compressor as a 20°F superheated vapor. From state 1 to state 9, the vapor is isentropically compressed (i.e., compressed at constant entropy) to the injection pressure. After which, the vapor mixed with the injected refrigerant continues to be isentropically compressed to discharge pressure from state 10 to state 2.

From state 2 to state 3, the vapor travels through part of the condenser which removes the superheat by cooling the vapor first, then the vapor travels through the remainder of the condenser, and is further cooled into a 15 °F subcooled liquid. The condensation process always occurs at essentially constant discharge pressure.

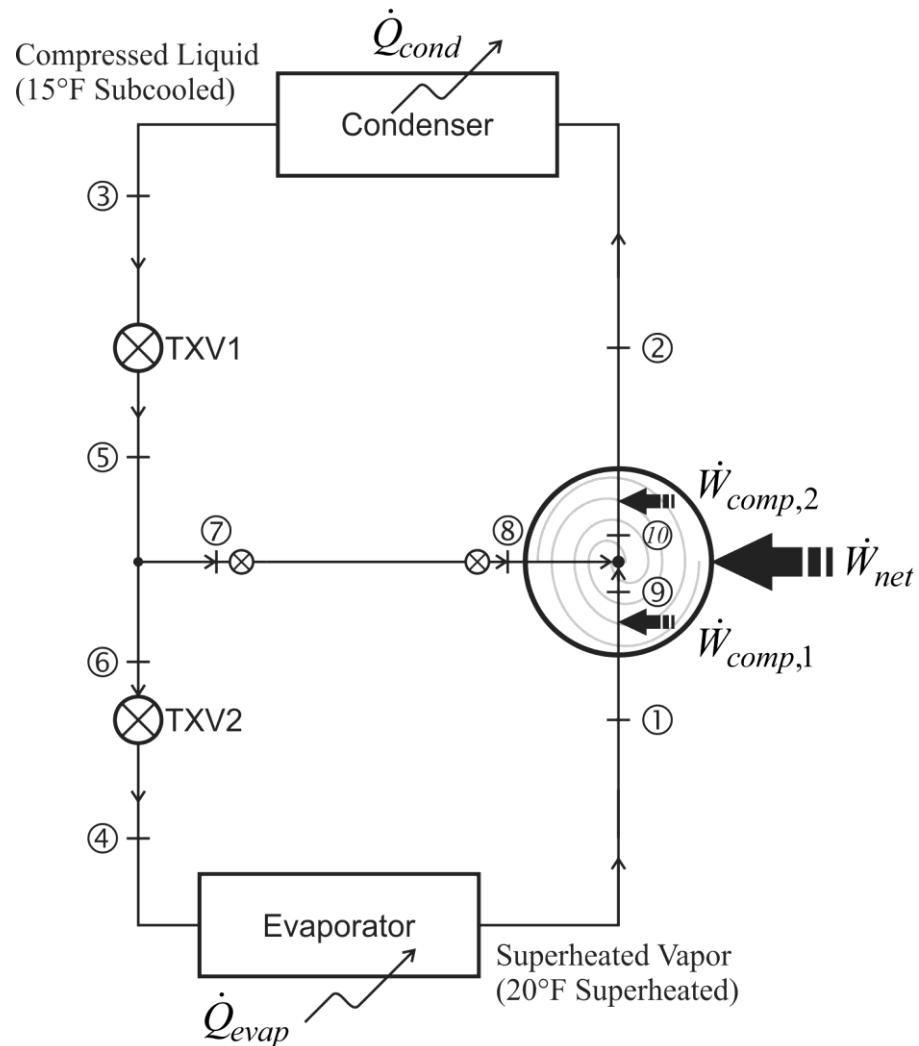


Figure 3.2: Refrigeration System Schematic Showing Hardware Components, Flow Connections and State Points.

From states 3 to state 5, the subcooled liquid refrigerant passes through the expansion valve and undergoes an abrupt decrease of pressure and temperature to the desired injection pressure. The subcooled liquid refrigerant becomes a two-phase mixture. Next, the refrigerant splits into two streams: a portion of the flow passes through another expansion valve from state 6 to state 4, expanding directly to the suction pressure, while the remaining flow is drawn

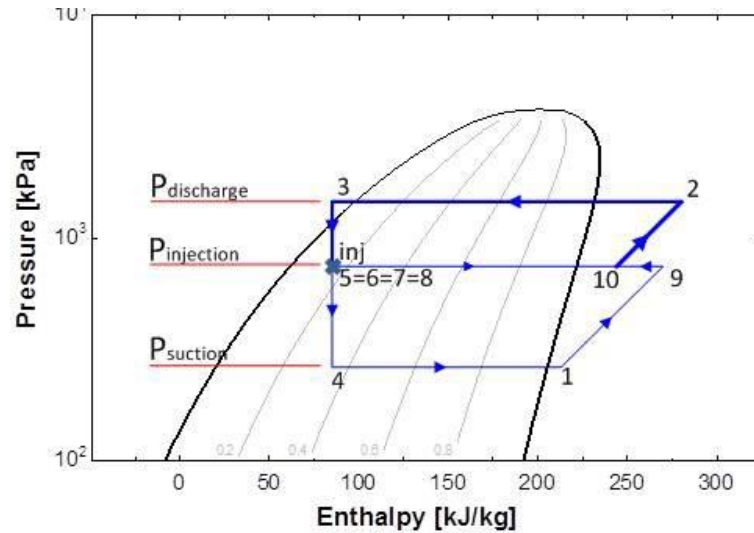


Figure 3.3: P-h Diagram of the Refrigeration System Performance with Controlled Injection Pressure.

off into injection line and directly injected to injection ports of the compressor.

Among state 8, state 9 and state 10, an adiabatic and isobaric homogeneous mixing process instantaneously occurs in the compressor on the injection pressure.

From states 4 to state 1, the cold and partially vaporized refrigerant travels through the coil or tubes in the evaporator where it is totally vaporized by warm air (from the space being refrigerated) that a fan circulates across the coil or tubes in the evaporator. The evaporator operates at essentially constant pressure and boils off all available liquid, thereafter adding 20°F of superheat to the refrigerant as a safeguard for the compressor as it cannot compress an incompressible fluid. The resulting refrigerant vapor returns to the compressor inlet at state 1 to complete the thermodynamic cycle.

It should be noted that the above discussion does not take into account real world items like frictional pressure drop in the system, internal irreversibility during the compression process, non-ideal gas behavior or adiabatic and isobaric homogeneous mixing process.

3.2.2 Model of the System

A model has been developed to predict the refrigeration system performance with controlled injection pressure over the range of anticipated operating conditions. The model is intended for use with R-410A as the working fluid and will be capable of simulating a variety of different compressors. The model should be easily adaptable to serve as a tool for evaluating the impact of compressor selection on system performance.

To accomplish this goal, the model uses manufacturer-supplied data to characterize the compressor performance. Copeland data is typically provided over a range of condensing and evaporating temperatures with a specified superheat at the compressor inlet and subcooling at the condenser exit. For a compressor without injection ports, manufacturers may report the expected cooling capacity, power consumption, current draw, mass flow rate, EER and isentropic efficiency of the compressor under each condition. However, the performance of a compressor designed to operate with economized vapor injection cannot be characterized as succinctly. Because of the economizer, the enthalpy of the refrigerant supplied to the evaporator no longer depends on the degree of subcooling at the condenser exit alone. Therefore, the manufacturer

must supply much more information to completely specify the conditions entering the evaporator and the injection line.

Although the manufacturer may supply information that can be used to determine the conditions entering the evaporator, additional information is needed to specify the state of the injected refrigerant. Therefore, providing a detailed description of the compressor performance is much more complex with injection.

It follows that completely describing the performance of a compressor with injection within the model would require significantly more inputs than describing a compressor without injection. However, it is desired to use the same model, and thus the same inputs, for compressors both with and without injection. Furthermore, the model must predict system performance with two-phase economized refrigerant injection, for which published compressor performance data is not available. Therefore, it was decided to characterize compressor performance in the model using isentropic efficiency alone. When the compressor inlet conditions (state 1) are known and the discharge pressure (state 2) is specified, the isentropic efficiency can be used to determine the discharge enthalpy:

$$\eta_s = \frac{h_{2s} - h_1}{h_2 - h_1}; \quad (3.2.1)$$

In this equation, h_{2s} represents the enthalpy of the refrigerant exiting an isentropic compression process from the inlet state to the exit pressure.

In order to apply this definition to a compressor with injection, the injection process is modeled as an adiabatic, isobaric mixing process between compressor stages, and Equation (3.2.1) is applied to each stage of the

compressor. For example, Equation (3.2.1) can be applied to a compressor with a single injection port by letting state 9 represent the state of the refrigerant in the compressor as it reaches the injection pressure. If state *inj* represents the state of the injected refrigerant, a mass and energy balance on the adiabatic mixing process can be used to determine the resulting state of the refrigerant in the compressor, which will be represented as state 10:

$$h_{10} = (1 - Ratio_m) \times h_9 + Ratio_m \times h_{inj}; \quad (3.2.2)$$

For convenience, the injection mass flow rate ratio, *Ratio_m*, is defined as the ratio of the injection mass flow rate, \dot{m}_{inj} , to the total mass flow rate existing in the compressor, \dot{m}_{total} :

$$Ratio_m \equiv \frac{\dot{m}_{inj}}{\dot{m}_{total}} \quad (3.2.3)$$

This ratio is defined relative to the total mass flow rate because it is assumed that injection will have a negligible impact on the volumetric efficiency or mass flow rate passing through the compressor. The injection mass flow rate ratio must be specified by the model user, if injection flow rates are available from the compressor manufacturer, or can be varied over a range of values to study the impact on system performance. Following the mixing process, the refrigerant continues to be compressed and (3.2.1) is used to calculate the resulting discharge state from the compressor.

Using the isentropic compressor efficiency and an adiabatic process to model the refrigeration system with injection simplifies the model considerably. In addition, the following assumptions are proposed:

1. Steady-state, steady flow conditions.
2. One-dimensional flow.
3. The compressor can be modeled using an isentropic efficiency.
4. The pressure drop through lines is negligible.
5. Compared to the heat transfer between the condenser and the heat sink, the heat transfer between the lines and the ambient is negligible.
6. The throttling devices are isenthalpic, with no work or heat transfer.
7. Kinetic and potential energy changes are small relative to changes in enthalpy and can be disregarded.
8. Any injection processes can be modeled as adiabatic, isobaric mixing processes.

In addition, the injection pressure ratio, $Ratio_p$, must be specified by the model user, is denoted as the ratio of the difference between injection pressure and inlet pressure, $P_{inj} - P_{inlet}$, to the difference between discharge pressure and suction pressure, $P_{outlet} - P_{inlet}$:

$$Ratio_p \equiv \frac{P_{inj} - P_{inlet}}{P_{outlet} - P_{inlet}}; \quad (3.2.4)$$

$Ratio_p$ can be varied over a range of values to conveniently study the impact on system performance.

The model was implemented using Engineering Equation Solver (Klein, 2009). It requires the user to specify the condensing and evaporating temperatures, degree of superheat at the compressor inlet and subcooling at the condenser outlet, compressor power input, mass flow rate and isentropic efficiency. The compressor manufacturer typically provides all of these

parameters on the performance sheet. Making the assumptions mentioned above, the model then will evaluate the thermodynamic properties at each state, the mass flow rate through each line in the model, and heat transfer rate in the condenser.

To clarify the modeling procedure, a flow chart is provided in Figure 3.4.

3.2.3 Sample Calculation and Model Feasibility Analysis

The same condition, where the Copeland compressor can achieve the highest efficiency in conventional refrigeration system, is picked up for a sample hand calculation of refrigeration system with injection pressure in the middle of the range from inlet pressure to outlet pressure. The sample calculation is intended to make sure there is no errors in the model codes by comparison between hand calculation results and simulation output. Meanwhile, this hand calculated process below shows the model procedure literally clear.

1. Conditions:

$T_{evap} = 45^\circ F$, $T_{cond} = 110^\circ F$, $\dot{m}_{total} = 670 \text{ lbm/hr}$, $\Delta T_{SH} = 20^\circ F$, $\Delta T_{SC} = 15^\circ F$. The compressor efficiency follows the correlations between η_{isen} and r_p of Equation 2.3.4.

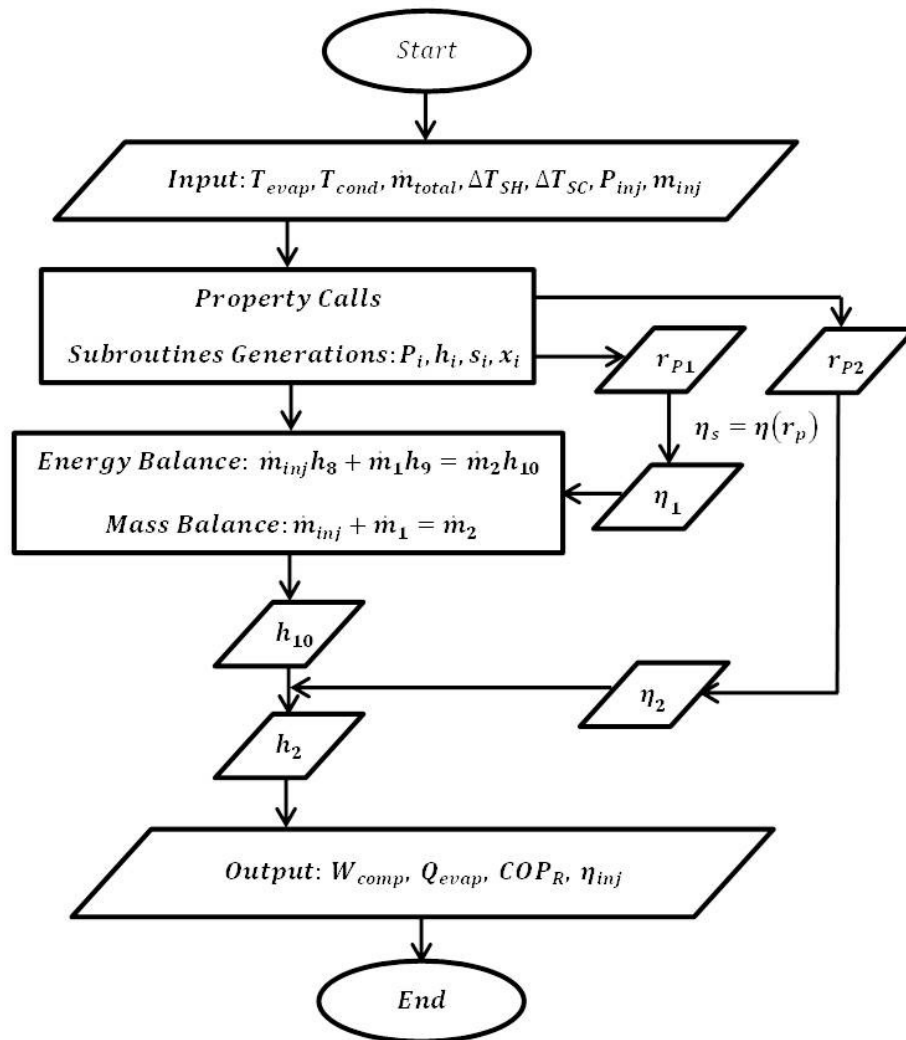


Figure 3.4: Flow Chart for The Model of Refrigeration Cycle with Two-Phase Flow Injection.

2. Calculations at State 1:

$$T_1 = T_{\text{evap}} + \Delta T_{\text{SH}} = 45 + 20 = 65^\circ \text{F}$$

$$P_1 = \text{Pressure}(\text{R410A}, T_{\text{evap}} = 45^\circ \text{F}, x = 1) = 144.8 \text{psia}$$

$$h_1 = \text{Enthalpy}(\text{R410A}, P_1 = 144.8 \text{psia}, T_1 = 65^\circ \text{F}) = 187.4 \text{Btu/lbm}$$

$$s_1 = \text{Entropy}(\text{R410A}, P_1 = 144.8 \text{psia}, T_1 = 65^\circ \text{F}) = 0.44 \text{Btu/lbm} * R$$

3. Specify the intermediate pressure ratio of $Ratio_p$ as 0.5. Calculations from State 1 to State 9:

$$Ratio_p = \frac{P_{inj} - P_1}{P_2 - P_1} \Rightarrow 0.5 = \frac{P_{inj} - 144.8}{P_2 - 144.8}$$

$$P_2 = \text{Pressure}(\text{R410A}, T_{\text{cond}} = 110^\circ \text{F}, x = 0) = 381.1 \text{psia}$$

$$P_{inj} = Ratio_p \times (P_2 - P_1) + P_1 = 0.5 \times (381.1 - 144.8) + 144.8 = 262.95 \text{psia}$$

$$r_{p1} = \frac{P_{inj}}{P_2} = \frac{262.95}{381.1} = 1.816$$

$$\eta_1 = -1.46 + 2.66 \times r_{p1} - 1.22 \times r_{p1}^2 + 0.27 \times r_{p1}^3 - 0.029 \times r_{p1}^4 + 0.00126 \times r_{p1}^5$$

$$= 0.6534$$

$$\eta_1 = \frac{h_{9s} - h_1}{h_9 - h_1} \Rightarrow 0.6534 = \frac{h_{9s} - 187.4 \text{Btu/lbm}}{h_9 - 187.4 \text{Btu/lbm}}$$

4. Calculations at State 9:

$$P_9 = P_{inj} = 262.95 \text{ psia}$$

$$h_{9s} = \text{Enthalpy}(R410A, P_9 = 262.95 \text{ psia}, s_1 = 0.44 \text{ Btu/lbm} \cdot R)$$

$$= 195 \text{ Btu/lbm}$$

$$h_9 = \frac{h_{9s} - h_1}{\eta_1} + h_1 = \frac{195 - 187.4}{0.6534} + 187.4 = 199.03 \text{ Btu/lbm}$$

$$T_9 = \text{Temperature}(R410A, P_9 = 262.92 \text{ psia}, h_9 = 199.03 \text{ Btu/lbm}) = 135.1^\circ F$$

5. Specify the injection mass flow rate ratio of $Ratio_m$ as 0.1. Calculations for mixing at the injection port:

$$Ratio_m = \frac{\dot{m}_{inj}}{\dot{n}_{total}} \Rightarrow 0.1 = \frac{\dot{m}_{inj}}{670}$$

$$\dot{m}_2 = \dot{m}_{total} = 670 \text{ lbm/hr}$$

$$\dot{m}_{inj} = 670 \times 0.1 = 67 \text{ lbm/hr}$$

$$\text{MassBalance} : \dot{m}_1 + \dot{m}_{inj} = \dot{m}_2$$

$$\dot{m}_1 = 670 - 67 = 603 \text{ lbm/hr}$$

$$\text{EnergyBalance} : \dot{m}_1 \times h_9 + \dot{m}_{inj} \times h_{inj} = \dot{m}_2 \times h_{10}$$

$$603 \text{ lbm/hr} \times 199.03 \text{ Btu/lbm} + 67 \text{ lbm/hr} \times h_{inj} = 670 \text{ lbm/hr} \times h_{10}$$

6. Calculations at State 3:

$$T_3 = T_{cond} - \Delta T_{SC} = 110 - 15 = 95^\circ F$$

$$P_3 = P_2 = 381.1 \text{ psia}$$

$$h_3 = \text{Enthalpy}(R410A, P_3 = 381.1 \text{ psia}, T_3 = 95^\circ F) = 110.4 \text{ Btu/lbm}$$

7. Calculations at State inj:

$$h_{inj} = h_3 = 110.4 \text{ Btu/lbm}$$

$$P_{inj} = \text{Ratio}_p \times (P_2 - P_1) + P_1 = 0.5 \times (381.1 - 144.8) + 144.8 = 262.95 \text{ psia}$$

$$T_{inj} = \text{Temperature}(R410A, P_{inj} = 262.95 \text{ psia}, h_{inj} = 110.4 \text{ Btu/lbm}) = 83.2 \text{ }^\circ \text{F}$$

$$x_{inj} = \text{Quality}(R410A, P_{inj} = 262.95 \text{ psia}, h_{inj} = 110.4 \text{ Btu/lbm}) = 0.06$$

8. Calculations at State 10:

$$h_{10} = \frac{\dot{m}_1 \times h_9 + \dot{m}_{inj} \times h_{inj}}{\dot{m}_2} = \frac{603 \times 199.03 + 67 \times 110.4}{670} = 190.167 \text{ Btu/lbm}$$

$$P_{10} = P_{inj} = 262.95 \text{ psia}$$

$$T_{10} = \text{Temperature}(R410A, P_{10} = 262.95 \text{ psia}, h_{10} = 190.167 \text{ Btu/lbm}) = 104.2 \text{ }^\circ \text{F}$$

$$s_{10} = \text{Entropy}(R410A, P_{10} = 262.95 \text{ psia}, h_{10} = 190.167 \text{ Btu/lbm})$$

$$= 0.432 \text{ Btu/lbm} * R$$

9. Calculations from State 10 to State 2.

$$r_{p2} = \frac{P_2}{P_{inj}} = \frac{381.1}{262.95} = 1.449$$

$$\eta_2 = -1.46 + 2.66 \times r_{p2} - 1.22 \times r_{p2}^2 + 0.27 \times r_{p2}^3 - 0.029 \times r_{p2}^4 + 0.00126 \times r_{p2}^5$$

$$= 0.5214$$

$$\eta_2 = \frac{h_{2s} - h_{10}}{h_2 - h_{10}} = 0.5214 = \frac{h_{2s} - 190.167 \text{ Btu/lbm}}{h_2 - 190.167 \text{ Btu/lbm}}$$

10. Calculations at State 2:

$$P_2 = \text{Pressure}(R410A, T_{\text{cond}} = 110^\circ F, x = 0) = 381.1 \text{ psia}$$

$$h_{2s} = \text{Enthalpy}(R410A, P_2 = 381.1 \text{ psia}, s_{10} = 0.432 \text{ Btu/lbm} * R)$$

$$= 194.9 \text{ Btu/lbm}$$

$$h_2 = \frac{h_{2s} - h_{10}}{\eta_2} + h_{10} = \frac{194.9 - 190.167}{0.5214} + 190.167 = 199.24 \text{ Btu/lbm}$$

$$T_2 = \text{Temperature}(R410A, P_2 = 381.1 \text{ psia}, h_2 = 199.24 \text{ Btu/lbm}) = 156^\circ F$$

11. Calculations at State 4:

$$h_4 = h_3 = 110.4 \text{ Btu/lbm}$$

$$P_4 = P_1 = 144.8 \text{ psia}$$

$$T_4 = \text{Temperature}(R410A, P_4 = 144.8 \text{ psia}, h_4 = 110.4 \text{ Btu/lbm}) = 44.8^\circ F$$

Table 3.1: State Point Properties of Model with Injection

State Pt No.(i)	$h_i(\frac{Btu}{lbm})$	$P_i(Psia)$	$s_i(\frac{Btu}{lbm \cdot R})$	$T_i(^{\circ}F)$	$x_i(-)$	$m_i(\frac{lbm}{hr})$
1	187.4	144.8	0.4397	65	SH	603
2	198.4	381.1	0.4377	153.7	SH	670
3	110.4	381.1	0.2841	95	CL	670
4	110.4	144.8	0.2872	44.85	0.2156	603
5	110.4	263	0.2848	83.16	0.0619	670
6	110.4	263	0.2848	83.16	0.0619	603
7	110.4	263	0.2848	83.16	0.0619	67
8	110.4	263	0.2848	83.16	0.0619	67
9	198.7	263	0.4463	134.1	SH	603
10	189.9	263	0.431	103.3	SH	670

12. Overall system

$$\dot{Q}_{evap} = \dot{m}_1 (h_1 - h_4) = 603 lbm/hr (187.4 - 110.4) Btu/lbm = 46431 Btu/hr$$

$$\dot{W}_{comp1} = \dot{m}_1 (h_9 - h_1) = 603 lbm/hr (199.03 - 187.4) Btu/lbm$$

$$= 7012.89 Btu/hr = 2055 W$$

$$\dot{W}_{comp2} = \dot{m}_2 (h_2 - h_{10}) = 670 lbm/hr (199.24 - 190.12) Btu/lbm$$

$$= 6078.91 Btu/hr = 1782 W$$

$$COP_R = \frac{\dot{Q}_{evap}}{\dot{W}_{comp1} + \dot{W}_{comp2}} = \frac{46431}{7012.89 + 6078.91} = 3.547$$

$$\eta_{inj} = \frac{\dot{m}_1 (h_{9s} - h_1) + \dot{m}_2 (h_{2s} - h_{10})}{\dot{m}_1 (h_9 - h_1) + \dot{m}_2 (h_2 - h_{10})}$$

$$= \frac{603 \times (195 - 187.4) + 670 \times (194.9 - 190.167)}{603 \times (199.03 - 187.4) + 670 \times (199.24 - 190.167)} = 0.5923$$

The EES program calculation results are summarized in the Table 3.1, for convenient reference and compared with hand calculation.

In this section, the feasibility of the model will be analyzed by proving that the coefficient of performance of the injection system equals to that of the conventional system when the injection pressure ratio and mass fraction go towards 1 and 0 respectively, $Ratio_p \rightarrow 1$ and $Ratio_m \rightarrow 0$, or when both the injection pressure ratio and mass fraction go towards 0, $Ratio_p \rightarrow 0$ and $Ratio_m \rightarrow 0$.

The COP of the conventional system on the same condition has been found in Chapter 2, which is 4.677, while the COP of the refrigeration system with injection equals to 4.657 when specifying the values of $Ratio_p$ and $Ratio_m$ as 0.9999 and 0.0001 in the EES program, or 4.655 when specifying the values of both $Ratio_p$ and $Ratio_m$ as 0.0001 in the EES program.

As such, the feasibility of the model of refrigeration system with injection has been proven reasonably.

3.2.4 Pre-Simulation Work

In order to investigate the two-phase fluid injection impact on the system, a well-planned approach is necessary to guide the simulation of the refrigeration cycle system in a scroll compressor with two-phase fluid injection. All the refrigeration system performance points are investigated under different intermediate pressure between input pressure and output pressure, different injection mass flow rate and different injection quality. A parametric investigation Table 3.2 will provide a clear vision of the whole investigation.

There are total 57 operating conditions in the manufacturer's data sheet. It will be a repetitive and time-consuming process to run all the cases. It is very

Table 3.2: Parametric Investigation Table

Intermediate Pressure Ratio	Mass Fraction	Injection Quality	Output
$Ratio_p = \frac{P_2 - P_1}{P_2}$	$Ratio_m = \frac{m_{inj}}{m}$	x	COP, η_{inj}
0.1	0.01 to 0.99	0 to 1	
0.3	0.01 to 0.99	0 to 1	
0.5	0.01 to 0.99	0 to 1	
0.7	0.01 to 0.99	0 to 1	
0.9	0.01 to 0.99	0 to 1	

necessary to select the desired conditions to focus the analysis. Because evaporating temperature is more relevant to cooling capacity, which is the concern in refrigeration system, the minimum and maximum compressor efficiency cases for each certain evaporating temperature are classified into Group A and Group B, respectively. The classification result is shown in Figure 3.5.

3.3 Model Results

3.3.1 Case Study of Minimum Compressor Efficiency Group

Group A represents the cases where compressor efficiencies reach the minimum values on each certain evaporating temperature in the feasible range. It includes two extreme cases:

1. A1: maximum compression ratio case including minimum evaporating temperature and minimum compressor efficiency;
2. A6: maximum condensing temperature case.

Three cases from Group A and one case from Group B were chosen to run the simulation, which are A1, A4, A6 and B1. Although B1 is maximum

Condensing Temp °F	Saturation Dew Pt Pressure psig	Evaporating Temp (°F)								
		-10	0	10	20	30	40	45	50	55
150	611						33100 5700 A6 575 5.8 58.4	36900 5600 A7 635 6.6 61.4	40900 5550 700	45100 5500 765
140	540					29400 5050 A5 475 5.8 57.0	36700 4920 585 7.5 63.4	40700 4870 645 8.4 66.0	44900 4810 705 9.3 68.2	49300 4770 770 10.3 70.0
130	475			25600 4460 A4 390 5.8 55.2	32500 4360 489 7.5 62.3	40200 4270 595 9.4 67.7	44300 4220 655 10.5 69.8	48800 4180 715 11.7 71.4	53500 4150 780 12.9 72.5	
120	417		22000 3950 A3 318 5.6 52.9	28400 3870 405 7.4 60.8	35600 3790 500 9.4 66.8	43500 3710 605 11.7 71.1	47900 3680 660 13.0 72.5	52500 3650 725 14.4 73.3	57500 3620 785 15.9 73.6	
110	364	18500 3500 A2 255 5.3 50.2	24500 3430 333 7.1 58.8	31000 3360 417 9.2 65.5	38400 3300 510 11.6 70.3	46700 3240 615 14.4 73.0	51500 3220 670 16.0 73.6	56000 3190 730 17.6 73.5	61500 3170 795 19.4 72.6	
100	316	15200 3090 A1 202 4.9 46.9	20700 3040 271 6.8 56.4	26700 2990 345 8.9 63.7	33500 2940 426 11.4 69.0	41100 2880 515 14.2 72.3	49800 2840 620 17.6 73.2	54500 2820 675 19.4 72.7	60000 2800 735 21.4 71.3	65500 2780 800 23.5 69.2
90	273	17200 2690 217 6.4 53.3	22700 2650 282 8.6 61.4	28800 2610 353 11.0 67.3	35700 2560 432 13.9 71.0	43600 2520 520 17.3 72.5	52500 2480 625 21.2 71.1	58000 2460 680 23.5 69.3	63000 2450 740 25.8 66.5	69000 2430 805 28.4 62.7
80	235	19000 2340 B1 227 8.1 58.5	24400 2300 B2 289 10.6 65.1	30600 2270 B3 358 13.5 69.4	37700 2230 B4 435 16.9 71.4	45900 2190 525 20.9 70.7	55500 2160 625 25.7 66.6	61000 2140 685 28.4 63.1	66500 2130 A8 745 31.3 58.5	72500 2110 A9 810 34.4 52.5

Figure 3.5: Demonstration of Group Setup.

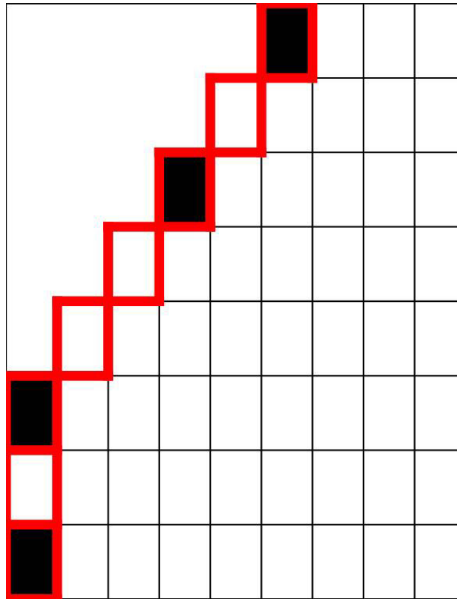


Figure 3.6: Location of the Potential Performance Improvement Group.

compressor efficiency case under -10°F evaporating temperature, it still has a very low compressor efficiency compared with the other cases. In sum, all the four representative cases have a common feature that they have very low compressor efficiency and very poor system performance in the conventional refrigeration system. They represent the blocks marked in the simplified data sheet of Figure 3.6 by highlighting in red with the name of potential performance improvement group.

After the simulation runs, the performance of the system at the four desired conditions is plotted in Figure 3.7. Additionally, the maximum COP that it can be achieved at each condition is also shown in the plot with the corresponding mass fraction and injection pressure ratio. In addition, the

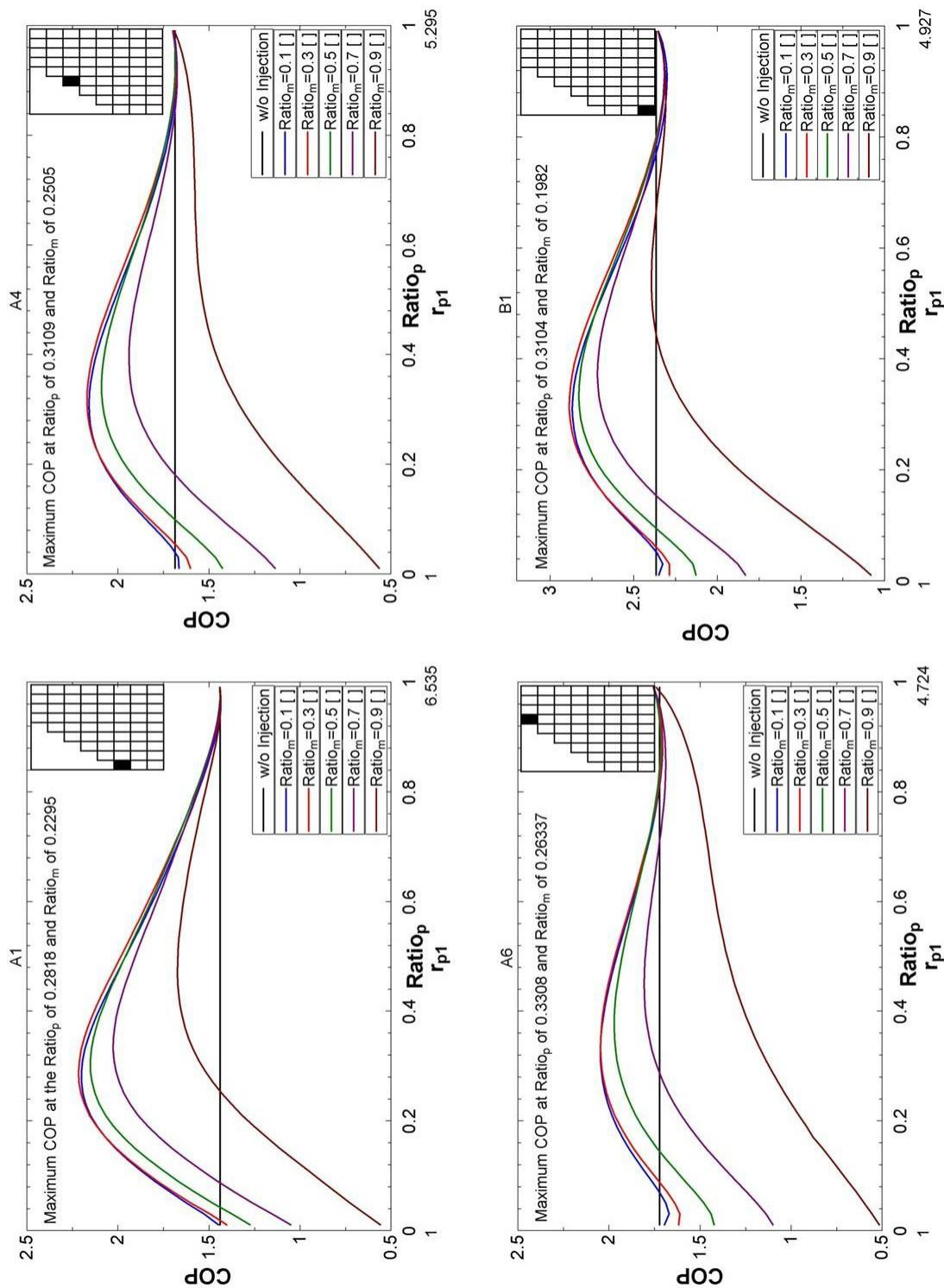


Figure 3.7: System Performance of Potential Performance Improvement Cases.

locations on the data sheet for each case are evidently marked in a simplified data sheet on the upper right corner of each plot.

It is obvious that potential performance improvement cases have very low compressor efficiency. Under the conditions of these cases, the refrigeration system with injection can achieve better performance than the conventional system in a wide range of injection pressure ratio if injecting refrigerant less than 70% mass fraction in this group. No additional benefit is attained in the high potential COP improvement group if injecting refrigerant more than 90% mass fraction.

On the operating condition of case A1, a maximum COP of 2.229 occurs when injecting refrigerant at 22.95% of mass fraction and holding the injection pressure ratio at 0.2818. The system performance is improved 55% over the conventional refrigeration system with the COP of 1.44 on the same operating condition. Similarly, for case A4, case A6 and case B1, each system performance is improved 29%, 19% and 23% by injection, respectively over their conventional refrigeration system performance.

Only when conventional refrigeration system has very low compressor efficiency and very poor system performance, can the cycle obtain benefit from injecting refrigerant into the compressor. The potential COP improvement in this group rises with the evaporating temperature decreasing and condensing temperature increasing. The case A1 has the best potential COP improvement over all the other cases with 55% performance improvement.

3.3.2 Case Study of Maximum Compressor Efficiency Group

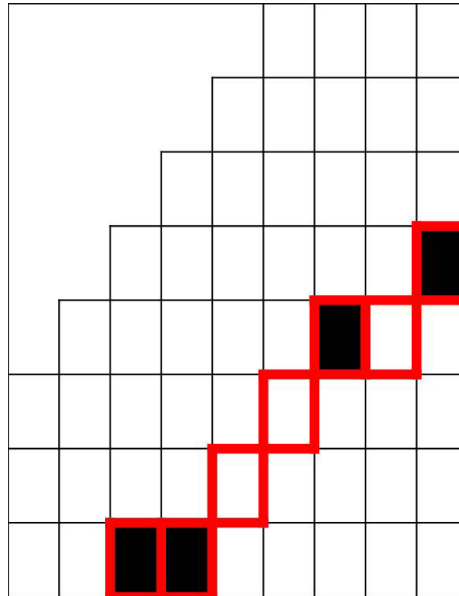


Figure 3.8: Location of the None Potential Performance Improvement Group.

Group B represents the cases where compressor efficiencies reach the maximum values on an each certain evaporating temperature in the feasible range. It includes two extreme cases:

B1: minimum evaporating temperature and condensing temperature case;

B7: maximum compressor efficiency case.

Four cases from Group B were chosen to run the simulation, which are B3, B4, B7 and B9. In sum, all the four representative cases have a common feature that they have high compressor efficiency and very excellent system performance in the conventional refrigeration system. They represent the blocks marked in the simplified data sheet of Figure 3.8 by highlighting in red with the name of none

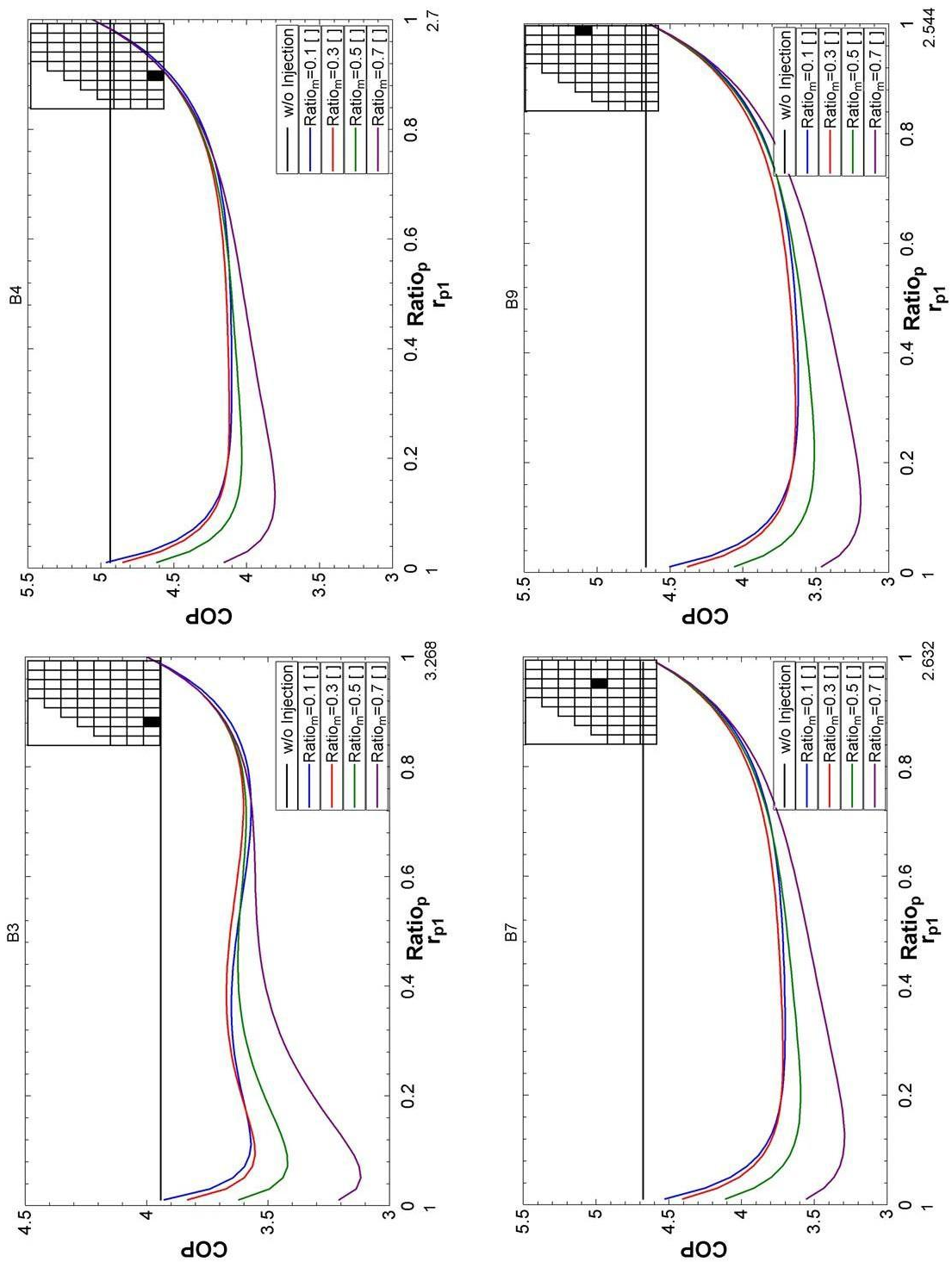


Figure 3.9: System Performance of the None Potential Performance Improvement Cases.

potential Performance improvement group.

After the simulation runs, the performances of the system on the four desired conditions is plotted in Figure 3.9. The locations on the data sheet for each case are evidently marked in a simplified data sheet on the upper right corner of each plot.

It is obvious that no potential performance improvement cases have very high compressor efficiency. Under the conditions of these cases, the refrigeration system with injection definitely got worse performance than conventional system in all the range of injection pressure ratio no matter how much refrigerant is injected. Injection would not get any benefits in this group.

When a conventional refrigeration system has a high compressor efficiency and good system performance, the cycle cannot obtain benefits from injecting refrigerant to compressor. However, the plots indicate that refrigeration system with injection trends to be close to conventional refrigeration system at around 0.3 of injection pressure ratio with the evaporating temperature decreasing and condensing temperature increasing.

3.3.3 Trend Prediction of Refrigeration System Performance with Injection

Two cases from Group A, one case from Group B and an additional case were chosen to run the simulation, which are A4, A9, B7 and X. Case A9 belongs to the minimum compressor efficiency group, representing the maximum evaporating temperature and minimum condensing temperature case. The additional case X is used to represent the case between the potential performance

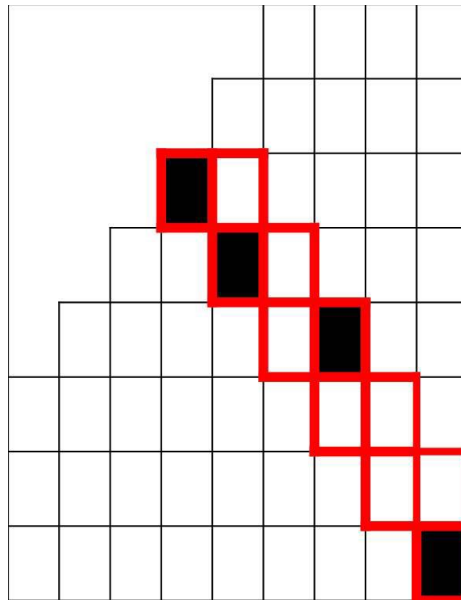


Figure 3.10: Location of the Cross Cases Group.

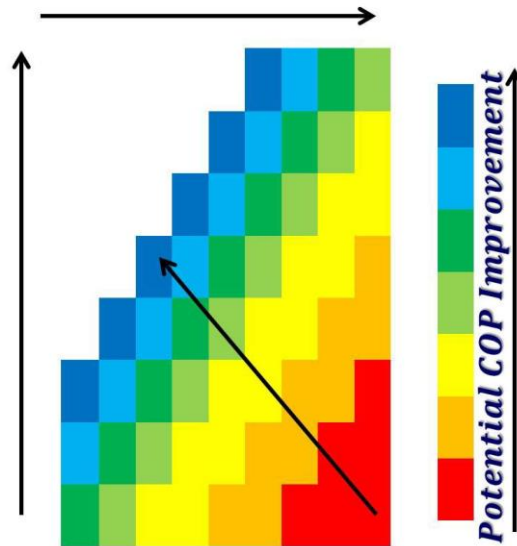


Figure 3.11: Trend Prediction of Refrigeration System Performance with Injection.

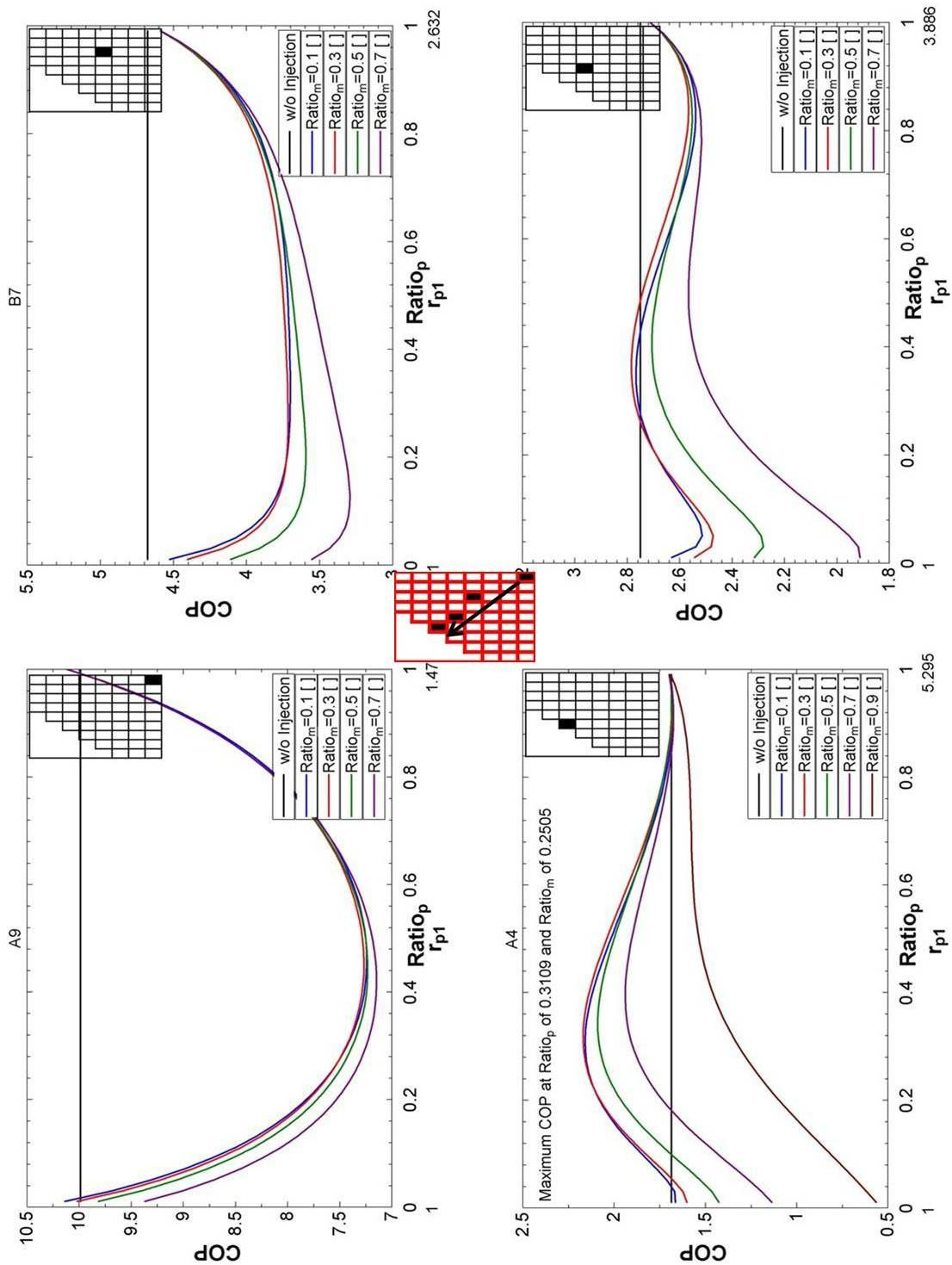


Figure 3.12: System Performance of Cross Cases.

improvement group and none potential performance improvement group.

In sum, all the four representative cases gather to form into a new group named with cross group. They represent the blocks marked in the simplified data sheet of Figure 3.10 by highlighting in red.

After the simulation runs, the performances of the system on the four desired conditions are plotted in Figure 3.12. The locations on the data sheet for each case are evidently marked in a simplified data sheet on the upper right corner of each plot.

These plots are indicated that the COP of the refrigeration system with injection undergoes a gradual process of rising with the evaporating temperature deceasing and condensing temperature increasing. The changing process is shown in Figure 3.11.

Chapter 4

Prediction of the Refrigeration System Performance with Controlled Injection Fluid Quality

After the investigation of a refrigeration system injected with controlled injection pressure on the conditions of the potential performance improvement group, a maximum COP of 2.229 occurs for the case A1 when injecting refrigerant at 22.95% of mass fraction and holding the injection pressure ratio at 0.2818. The system performance is improved 55% over the conventional refrigeration system with the COP of 1.44 for the same operating conditions. Similarly, for case A4, case A6 and case B1, each system performance is improved by injection 29%, 19% and 23%, respectively over their conventional refrigeration system performance. (See Figure 3.7).

However, system performance in previous model has been improved by injecting two-phase refrigerant fluid, which may cause compressor failures. Essentially, slugging is the result of trying to compress liquid refrigerant in the compressor. HVAC&R technicians have been aware of compressor failures caused by slugging for many years. It used to be a much greater problem, and more emphasis was put on it. Today many compressor failures are still attributed to slugging.

A further investigation on the potential performance improvement group is

conducted based on a refrigeration system injected with controlled injection fluid quality. This model is intend to investigate the optimum refrigeration system performance with injection, taking into account the slugging problem. The slugging problem is addressed by maintaining a minimum degree of superheat in the compressor.

4.1 Refrigeration System Injected with Controlled Injection Quality

In order to keep compressors from slugging, it is necessary to maintain the refrigerant mixture temperature within the scroll compressor at least 20°F above the saturation temperature at the injection pressure, which is widely accepted by HVAC&R manufacturers.

To further investigate the effect of injection on the conventional refrigeration system with this constraint of 20°F, after the refrigerant comes out of condenser, it passes through an expansion valve used to control the injection pressure, then it is heated to the desired quality by an intermediate heat exchanger before injected to injection ports on the compressor. The refrigeration system is schematically shown in Figure 4.1.

4.1.1 Thermodynamic Analysis of the System

The thermodynamics of a refrigeration system injected with controlled injection fluid quality can be analyzed on a pressure versus enthalpy diagram as ideally depicted in Figure 4.2. At state 1 in the diagram, the circulating refrigerant

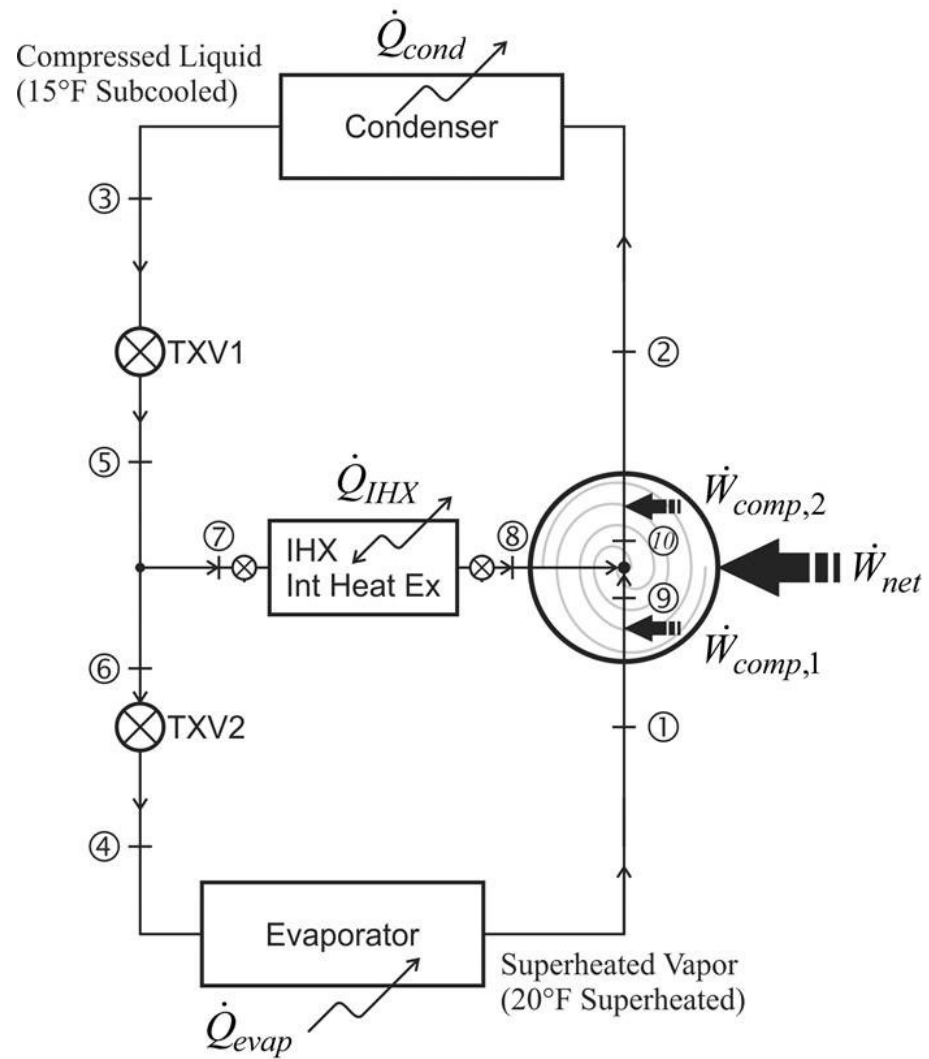


Figure 4.1: Refrigeration System Schematic Showing Hardware Components, Flow Connections and State Points.

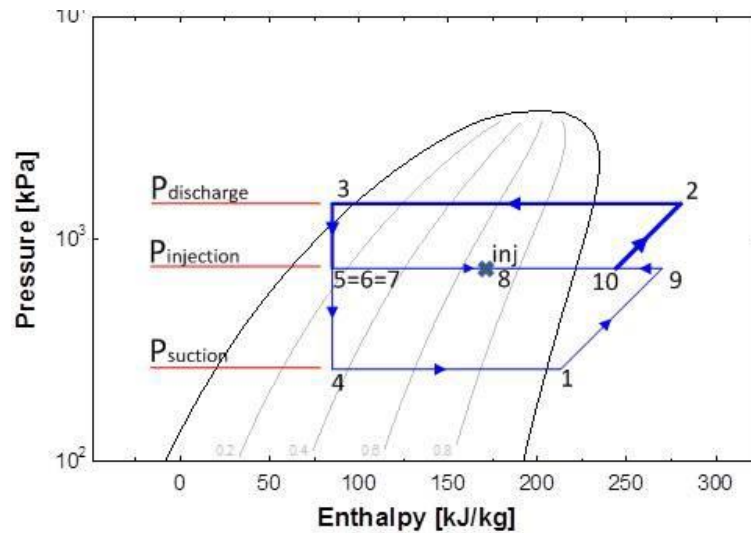


Figure 4.2: P-h Diagram of the Refrigeration System Performance with Controlled Injection Quality.

enters the compressor as a 20°F superheated vapor. From state 1 to state 9, the vapor is isentropically compressed (i.e., compressed at constant entropy) to the injection pressure. After which, the vapor mixed with the injected refrigerant continues to be isentropically compressed to the discharge pressure from state 10 to state 2.

From state 2 to state 3, the vapor travels through a part of the condenser which removes the superheat by cooling the vapor travels through the remainder of the condenser and is condensed to a 15°F subcooled liquid. The condensation process occurs at essentially constant pressure.

From state 3 to state 5, the subcooled liquid refrigerant passes through the expansion valve and undergoes an abrupt decrease of pressure and temperature to the desired injection pressure. The subcooled liquid refrigerant becomes two-phase mixture. Next, the refrigerant splits into two streams: a portion of the flow

passes through another expansion valve from state 6 to state 4, expanding directly to the suction pressure, while the remaining refrigeration flow is drawn off into an injection line and heated in an intermediate heat exchanger (IHX) from state 7 to state 8 to control the injection fluid quality prior to injection into the ports of the compressor.

Among state 8, state 9 and state 10, an adiabatic and isobaric homogeneous mixing process occurs in the compressor at the injection pressure.

From state 4 to state 1, the cold and partially vaporized (i.e. low quality) refrigerant travels through the evaporator coil or tubes, where it is totally vaporized by warm air (from the space being refrigerated). A fan circulates air across the coil or tubes in the evaporator. The evaporator operates at essentially constant pressure and boils off all available liquid thereafter adding 20°F of superheat to the refrigerant as a safeguard for the compressor, as it cannot tolerate any incompressible fluid. The resulting refrigerant vapor returns to the compressor inlet at state 1 to complete the thermodynamic cycle.

It should be noted that the above discussion is based on some assumptions which does not take into account real world items like frictional pressure drop in the system, internal irreversibility during the compression process, non-ideal gas behavior or adiabatic and isobaric homogeneous mixing process.

4.1.2 Model of the System

A modification has been made to the model of the refrigeration system injected with controlled injection pressure. An intermediate heat exchanger (IHX)

is installed into the injection line. The injected refrigerant fluid quality can be controlled by heating the injection line. The updated simulation model has the function to predict refrigeration cycle performance over the range of anticipated operating conditions, using R-410A as the working fluid and will be capable of testing a variety of different compressors with a safeguard to keep them from slugging.

The model uses manufacturer-supplied data from Copeland to characterize the compressor performance. This data is typically provided over a range of condensing and evaporating temperatures with a specified superheat at the compressor inlet and subcooling at the condenser exit. For a compressor without injection ports, manufacturers report the expected cooling capacity, power consumption, current draw, mass flow rate, EER and isentropic efficiency of the compressor under each operating condition. However, the performance of a compressor designed to operate with economized vapor injection cannot be characterized as succinctly. Because of the economizer, the enthalpy of the refrigerant supplied to the evaporator no longer depends on the degree of subcooling at the condenser exit alone. Therefore, the manufacturer must supply much more information to completely specify the conditions entering the evaporator and the injection line.

Although the manufacturer may supply information that can be used to determine the conditions entering the evaporator, additional information is needed to specify the state of the injected refrigerant. Therefore, providing a detailed description of the compressor performance is much more complex with injection.

It follows that completely describing the performance of a compressor with injection within the model would require significantly more inputs than describing a compressor without injection. However, it is desired to use the same model, and thus the same inputs, for compressors both with and without injection. Furthermore, the model must predict system performance with two-phase economized refrigerant injection, for which published compressor performance data is not available. Therefore, it was decided to characterize compressor performance in the model using isentropic efficiency alone, which was explained in the section of model of the system in Chapter 3.

In order to control the injection fluid quality, an internal heat exchanger is employed in the injection line of the model. When the IHX inlet (state 7) and the heat transferred into injection line is specified, the injection fluid quality can be determined (state 8) in the following equations:

$$\dot{Q}_{IHX} = Ratio_m \times \dot{m}_{total} (h_8 - h_7); \quad (4.1.1)$$

$$x_8 = Quality(R410A, P_8, h_8); \quad (4.1.2)$$

In this equation, x_8 represents the quality of the refrigerant exiting the IHX, which also means the injection fluid quality. (See Figure 4.1).

Using the isentropic compressor efficiency and an adiabatic process to model the refrigeration system with injection simplifies the model considerably. In addition, the same assumptions as the model in Chapter 3 are applied to the model of the refrigeration system with controlled injection fluid quality.

The model was implemented using Engineering Equation Solver (Klein, 2009). It requires the user to specify the condensing and evaporating

temperatures, degree of superheat at the compressor inlet and subcooling at the condenser outlet, compressor power input, mass flow rate and isentropic efficiency. The compressor manufacturer typically provides all of these parameters on the published performance sheet. Making the assumptions mentioned above, the model will then calculate the thermodynamic properties at each state, the mass flow rate through each line in the model, and heat transfer rate in the condenser.

The flow chart has been provided in Figure 3.4 of Chapter 3, which represents the modeling procedure for the refrigeration system with controlled injection fluid quality.

4.2 Model Results

4.2.1 Continuous Case Study of Minimum Compressor Efficiency Group

Temperature Profile at Injection Port in the Compressor

The same as the inlet situation that refrigerant enters the compressor as a 20°F superheated vapor, it is also necessary to maintain the refrigerant mixture temperature within the scroll compressor at least 20°F above the saturation temperature at the injection pressure, to keep it from slugging.

The way the injection fluid quality being controlled is to simply use an intermediate heat exchanger to heat the injection fluid. The desired injection fluid quality can be achieved by heating to the fluid. It is easy to determine the relationship between refrigeration system performances with injection fluid

quality.

The potential system performance improvement group in the previous model has been improved by injecting two-phase refrigerant fluid, but risks putting the compressor into a slugging situation. The temperature at the injection port in the compressor is straightforward to determine if the mixed refrigerant in the compressor stays in the superheated region. The temperature profiles at the injection port will display a clear vision of how the mixed refrigerant in the compressor changes with the addition of heat and where the constraint appears in the performance profiles.

After the runs of program on the same conditions as the four cases' in the potential performance improvement group, the temperature profiles at the injection port by different amounts of heat transfer are shown in the Figure 4.3 below. The constraint has been marked on the temperature profiles as a dashed line.

The plots indicate that a certain heat should be transferred into the injected refrigerant fluid to keep it at a 20°F superheated status. More heat should be transferred into if the injected refrigerant fluid stays in a low compression ratio; otherwise, less heat is required even no heat if the fluid stays in a high compression ratio. Therefore, there must be a value of the heat transfer that not only satisfies the constraint but also corresponds to an optimum system performance.

Performance of the Refrigeration System Performance with Controlled Injection Fluid Quality

The performance of the refrigeration system injected with controlled injection fluid quality is investigated using the new model based on the four cases of A1, A4, A6 and B1 in the potential performance improvement group. The result is displayed in the plot shown in Figure 4.4.

The blue lines in the plots represent the optimum performance of the refrigeration system with controlled injection pressure over different compression ratios. It is illustrated that the system performance is degraded by heating the injected refrigerant fluid. So it would not be necessary to transfer too much heat into the injection line. The dashed line in the plot represent the system performance of the refrigeration system on the constraint that keeping compressor from slugging.

The maximum COP for the refrigeration system injected with controlled injection fluid quality will appear at the peak of the dashed line. For the case A1, the maximum COP of 2.063 occurs when injecting refrigerant at 22.95% of mass fraction, holding the injection pressure ratio at 0.3232 and transferring the heat in at 1862 Btu/hr. The system performance is improved 43% over the conventional refrigeration system with the COP of 1.44 for the same operating condition. Nearly 12% performance improvement is sacrificed to keep the compressor from slugging.

Similarly, for case A4, case A6 and case B1, each system performance is improved 19%, 11% and 14% by injection, respectively over their conventional refrigeration system performance, as well as nearly 10%, 8% and 9% performance

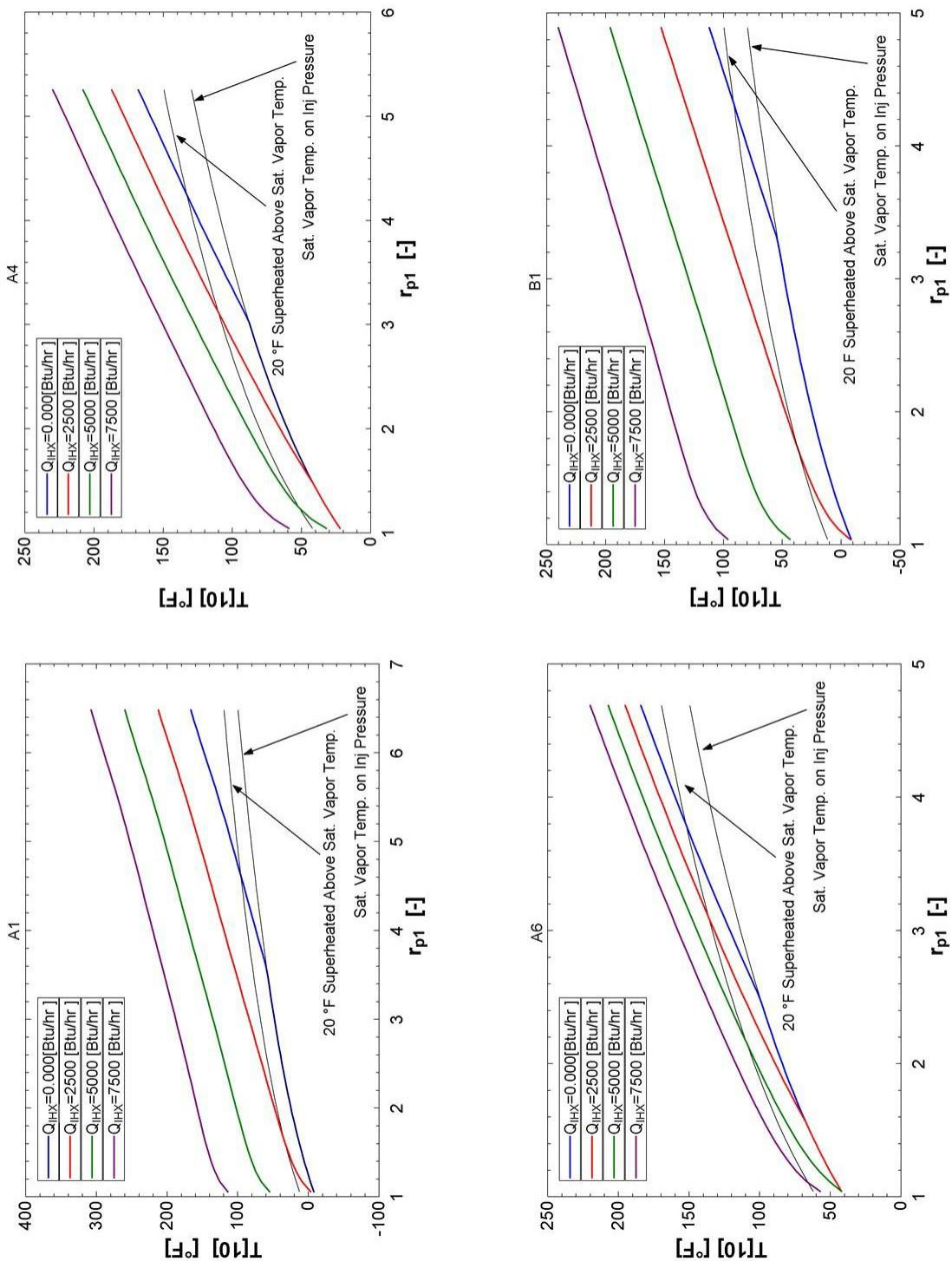


Figure 4.3: Temperature Profiles at Injection Port by Different Amounts of Heat transfer.

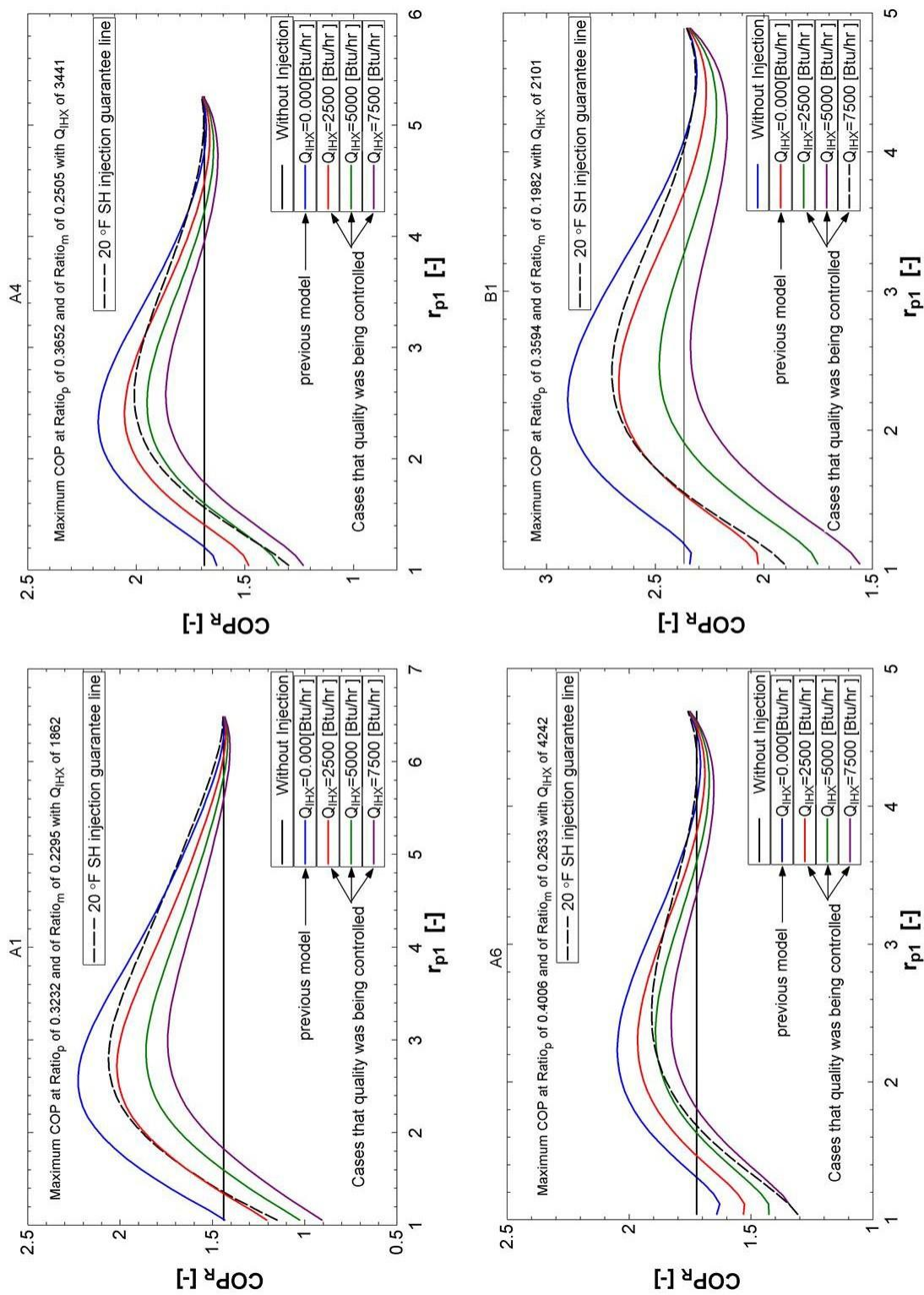


Figure 4.4: Cycle Performance Improvement with Controlled Injection Quality

improvement have been sacrificed respectively, to keep the compressor from slugging.

Injection Fluid Quality

In addition, injection fluid quality for each of the cases is shown on the plot of Figure 4.5. The plot illustrates how the injection fluid quality changes with heat transfer.

According to the condition where the refrigeration system with injection achieve the best performance, the injection fluid quality values for the four cases of A1, A4, A6 and B1 can be found on the plots, being 0.6123, 0.64, 0.6225 and 0.6138, respectively. The optimum refrigeration system performance with injection occurs when the injection quality ranges from 0.61 to 0.64.

4.2.2 Sensitivity Analysis of Coefficient of Performance of the Refrigeration System with Two-Phase Fluid Injection

The usefulness of any mathematical model depends in part on the accuracy and reliability of its input. Yet, because all models are imperfect abstractions of reality, and because precise input data are rarely if ever available, all output values are subject to inaccuracies. As such, uncertainty and sensitivity analysis is necessary to understand the mathematical model and behavior of the system.

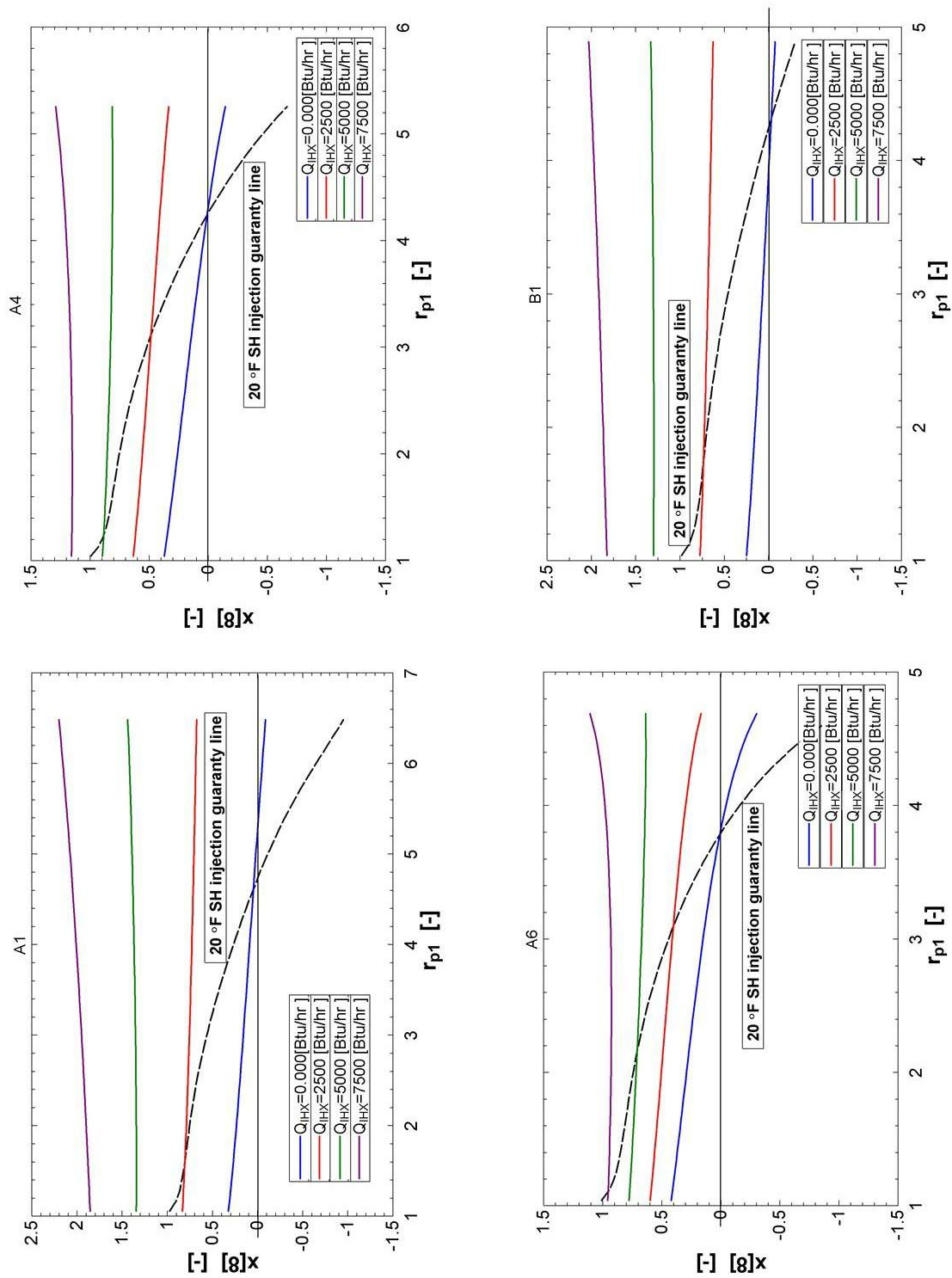


Figure 4.5: Injection Quality Profile.

Table 4.1: Sensitivity Analysis of Optimal Results of Case A1 ($T_{evap} = -10^\circ F | T_{cond} = 100^\circ F$)

Variable±Uncertainty	Partial Derivative	% of Uncertainty
$COP_R = 2.063 \pm 0.027$		
$Ratio_m = 0.2295 \pm 10\%$	$\partial COP_R / \partial Ratio_m = -0.5692$	23.41%
$Ratio_p = 0.3232 \pm 10\%$	$\partial COP_R / \partial Ratio_p = -0.3975$	22.65%
$x_{ini} = 0.6123 \pm 10\%$	$\partial COP_R / \partial x_{ini} = -0.3238$	53.94%

Table 4.2: Sensitivity Analysis of Optimal Results of Case A4 ($T_{evap} = 20^\circ F | T_{cond} = 130^\circ F$)

Variable±Uncertainty	Partial Derivative	% of Uncertainty
$COP_R = 2.01 \pm 0.02799$		
$Ratio_m = 0.25 \pm 10\%$	$\partial COP_R / \partial Ratio_m = -0.6223$	30.90%
$Ratio_p = 0.3652 \pm 10\%$	$\partial COP_R / \partial Ratio_p = -0.3218$	17.63%
$x_{ini} = 0.64 \pm 10\%$	$\partial COP_R / \partial x_{ini} = -0.3137$	51.46%

Table 4.3: Sensitivity Analysis of Optimal Results of Case A6 ($T_{evap} = 40^\circ F | T_{cond} = 150^\circ F$)

Variable±Uncertainty	Partial Derivative	% of Uncertainty
$COP_R = 1.908 \pm 0.02614$		
$Ratio_m = 0.2633 \pm 10\%$	$\partial COP_R / \partial Ratio_m = -0.5668$	32.59%
$Ratio_p = 0.4006 \pm 10\%$	$\partial COP_R / \partial Ratio_p = -0.3053$	21.89%
$x_{ini} = 0.6225 \pm 10\%$	$\partial COP_R / \partial x_{ini} = -0.2833$	45.52%

Table 4.4: Sensitivity Analysis of Optimal Results of Case B1 ($T_{evap} = -10^\circ F | T_{cond} = 80^\circ F$)

Variable±Uncertainty	Partial Derivative	% of Uncertainty
$COP_R = 2.701 \pm 0.02885$		
$Ratio_m = 0.1982 \pm 10\%$	$\partial COP_R / \partial Ratio_m = -0.7163$	24.22%
$Ratio_p = 0.3594 \pm 10\%$	$\partial COP_R / \partial Ratio_p = -0.3128$	15.19%
$x_{ini} = 0.6138 \pm 10\%$	$\partial COP_R / \partial x_{ini} = -0.3659$	60.60%

Uncertainty analysis, also called sensitivity analysis, is the study of how the uncertainty in the output of a mathematical model or system can be apportioned to different sources of uncertainty in its inputs. Uncertainty analysis has a greater focus on uncertainty quantification and propagation of uncertainty.

For the model of the refrigeration system with injection, the system performance is assessed by COP, which is the output of the mathematical model. The system performance can be apportioned to three sources of uncertainty in its inputs of injection mass fraction, injection pressure ratio and injection fluid quality. (i.e., the independent variables in the model).

Therefore, uncertainty analysis of coefficient of performance on refrigeration system with injection is conducted through EES program on the four cases in the potential performance improvement group. The results are shown in the Tables of 4.1, 4.2, 4.3 and 4.4, respectively:

In sum, the injection fluid quality has a significant effect on the refrigeration system with injection. The injection mass fraction has a much less effect than injection fluid quality but a little more effect than injection pressure ratio on the system performance.

Note that the independent variables are varied by 10 percent, yet the variation of COP is only approximately 1%.

Chapter 5

Summary and Conclusions

5.1 Summary

There are many opportunities to improve the performance of vapor compression equipment through the use of advanced compression techniques such as multi-stage compression or compression with refrigerant injection. The completed work presented in this paper represents significant progress towards understanding the potential benefits and limits of a refrigeration system modified to use these compression techniques with two-phase refrigerant fluid injection.

A model of the conventional compression cycle was developed to serve as a basis for investigating cycles with two-phase injection. In order to analyze the model practically, the Copeland scroll compressor system data sheet provided a range of anticipated operating conditions with a specified superheat at the compressor inlet and subcooling at the condenser exit, the working fluid R-410a, the expected cooling capacity, power consumption, current draw, mass flow rate, EER and isentropic compressor efficiency under selected operating conditions. Based on all above, the basic cycle performance analysis was theoretically simulated using EES software to conclude the correlation between the compressor efficiency and the compression pressure ratio as well as the correlation between mass flow rate and evaporating temperature.

The development of the basic cycle model with two-phase refrigerant fluid

injection provided a means for investigating the performance of the refrigeration system with two-phase refrigerant fluid injection, and confirmed the ability of this modifications to improve cycle performance.

The developed basic cycle model with two-phase refrigerant fluid injection was numerically analyzed, considering that the refrigerant exiting the condenser passes through an expansion valve used to control the injection pressure, then it is directly injected into the injection ports on the compressor. The analysis indicated the operating conditions on the data sheet where the injection has the best potential to improve the system performance and also investigated the conditions where the optimum system performance occurs.

To further investigate the effect of injection on the conventional compression cycle with the constraint of maintaining the refrigerant mixture within the compressor at least 20°F above the saturation temperature, it is considered that the refrigerant is heated to the desired quality before injected to injection ports on the compressor. Similarly, the developed basic cycle model with two-phase refrigerant fluid injection was numerically analyzed again to find the conditions where the optimum system performance occurs. Additionally, an uncertainty analysis of coefficient of performance was conducted on the refrigeration system with two-phase fluid injection.

5.2 Conclusions

The optimum benefits of two-phase injection are most pronounced for cycles operating across a large temperature difference, with up to a 55% improvement in COP at an evaporating temperature of -10°F and a condensing temperature of 100°F , by holding the injection pressure ratio at 0.2818 and injection mass fraction at 0.2295. Considering the constraint of maintaining the refrigerant mixture temperature within the compressor at least 20°F above the saturation temperature at the injection pressure, the optimum benefits of the two-phase injection are still significant for cycles operating across the same large temperature difference, with up to a 43% improvement in COP by increasing the injection mass pressure ratio to 0.3232 and holding the injection mass fraction at 0.2295, as well as the injection quality at 0.6123.

By sensitivity analysis on the simulation of the refrigeration system with two-phase fluid injection, the injection fluid quality has a significant effect on the refrigeration system COP. The injection mass fraction has a much less effect than injection fluid quality but a little more pronounced than injection pressure ratio on the system performance. For the operating condition where the refrigeration system with two-phase fluid injection achieve the best potential COP improvement, varying the independent variables (injection mass fraction, injection pressure ratio and injection fluid quality) by $\pm 10\%$, the uncertainty of the injection mass fraction, injection pressure ratio and injection fluid quality are 23.41%, 22.65% and 53.94%, respectively, yet the variation of COP is only approximately 1.3%.

Bibliography

- [1] “Refrigeration,” URL: <https://en.wikipedia.org/wiki/Refrigeration>.
- [2] “Online product information,” URL:
<https://opi.emersonclimate.com/was.extension.opi.web/OPIServlet>.
- [3] R. J. G. Gordan J. Gerber and J. H. Karian, “Performance test code on compressors and exhausters,” *The American Society of Mechanical Engineers*, 1998.
- [4] W. Bianchi and E. Winandy, “Performance improvements in commercial refrigeration with vapour injected scroll compressors,” *Emerson Climate Technologies*.
- [5] “Residential energy consumption survey, 2005,” URL:
<http://www.eia.doe.gov/emeu/recs/>.
- [6] H. H. Cho and Y. Kim, “Experimental study on an inverter-driven scroll compressor with an injection system,” *International Compressor Engineering Conference*, p. 1463, 2000.
- [7] Y. M. F. Liu, H. Huang and R. Zhuang, “An experimental study on the heat pump water heater system with refrigerant injection,” In: *Proceedings of International Refrigeration and Air Conditioning Conference at Purdue*, pp. 2211–2216, 2008.
- [8] Y. H. Xudong Wang and R. Radermacher, “Performance investigation of

refrigerant vapor-injection technique for residential heat pump systems,” *International Refrigeration and Air Conditioning Conference at Purdue, 2008*.

- [9] Y. H. Xudong Wang and R. Radermacher, “Two-stage heat pump system with vapor-injected scroll compressor using r410a as a refrigerant,” *International Journal of Refrigeration*, vol. 32, pp. 1442–2451, 2009.
- [10] K. S. H. K. H. Yamazaki, T. Itoh and M. Kawada, “High performance scroll compressor with liquid refrigerant injection,” *International Compressor Engineering Conference*, p. 1596, 2002.
- [11] V. A. Jon Winkler, Xudong Wang and R. Radermacher, “Simulation and validation of a two-stage flash tank cycle using r410a as a refrigerant,” *International Refrigeration and Air Conditioning Conference at Purdue, 2008*.
- [12] J. G. Jain Siddharth and B. Clark, “Vapor injection in scroll compressors,” *International Compressor Engineering Conference at Purdue, 2004*.
- [13] Z. Liu and W. Soedel, “An investigation of compressor slugging problems,” *International Compressor Engineering conference at Purdue*, pp. 433–440, 1994.
- [14] Z. Liu and W. Soedel, “A mathematical model for simulating liquid and vapor two-phase compression processes and investigating slugging problems in compressors,” *HVACR Research*, vol. 1, no. 2, pp. 90–109, 1995.
- [15] J. E. B. Margaret M. Mathison and E. A. Groll, “Approaching the performance limit for economized cycles using simplified cycles,” *International Journal of Refrigeration*, vol. 45, pp. 67–72, 2014.

- [16] J. E. B. Margaret M. Mathison and E. A. Groll, "Performance limit for economized cycle with continuous refrigerant injection," *International Journal of Refrigeration*, vol. 34, no. 1, pp. 234–242, 2011.
- [17] R. Rajendran and A. Nicholson, "Air-conditioning, heating, and refrigeration institute (ahri) low-gwp alternative refrigerants evaluation program (low-gwp arep)," *Emerson Climate Technologies, Inc.*, 2013

APPENDIX I.

EES CODES FOR CONVENTIONAL VAPOR COMPRESSION REFRIGERATION CYCLE

"Rui Gu Creates The File On December 5, 2015"

" Maximum Compressor Efficiency Case Verification"

m_dot = 670 [lbm/hr]; T_evap = 45 [F]; T_cond = 110 [F];
W_data = 3220 [W]; Q_data = 51500 [Btu/hr]; eta_data = 0.736 [-]

"The Conventional Vapor-Compression Refrigeration Cycle Model Verification

Given Information:"

WF\$ = 'R410a';

P[1] = Pressure(WF\$, T=T_evap, x=1); T[1] = T_evap + 20 [F] " Compressor Inlet, 20 Degree Superheated"

P[2] = P[3] " Compressor Outlet and Condenser Inlet"

P[3] = Pressure(WF\$, T=T_cond, x=0); T[3] = T_cond - 15 [F] " Condenser Outlet, 15 Degree Subcooled"

P[4] = P[1] " Evaporator Suction Pressure"

r_p = P[2] / P[1] "Overall Pressure Ratio"

eta_s = eta_data

"Energy Balance, Compressor {1 -> 2}"

Q_dot_comp + W_dot_comp*convert(W, Btu/hr) + m_dot * (DELTAh_1_2 + DELTAke_1_2 + DELTApe_1_2) =
DELTAE_sys_comp

" Assumptions:1) Steady State Operation; 2) Adiabatic, Reversible Compression;"

" 3) Negligible Changes in Kinetic and Potential Energy."

" DELTAE_sys_comp = 0 [Btu/hr]; Q_dot_comp = 0 [Btu/hr];

" DELTAke_1_2 = 0 [Btu/lbm]; DELTApe_1_2 = 0 [Btu/lbm]

" Property/Function Calls:"

" DELTAh_1_2 = h[1] - h[2]

" h[1] = Enthalpy(WF\$,P=P[1],T=T[1]);

" s[1] = Entropy(WF\$,P=P[1],T=T[1]);

" eta_s=(h[1]-h_2s)/(h[1]-h[2])

" h_2s = Enthalpy(WF\$,P=P[2],s=s[1]);

" T[2] = Temperature(WF\$,P=P[2],h=h[2])

" s[2] = Entropy(WF\$,P=P[2],h=h[2])

"

"

"Energy Balance, Condenser {2 -> 3}"

Q_dot_cond + W_dot_cond*convert(W, Btu/hr) + m_dot * (DELTAh_2_3 + DELTAke_2_3 + DELTApe_2_3) =
DELTAE_sys_cond

" Assumptions:1) Steady State Operation; 2) No Work Interactions;"

" 3) Negligible Changes in Kinetic and Potential Energy."

" DELTAE_sys_cond = 0 [Btu/hr]; W_dot_cond = 0 [W]

" DELTAke_2_3 = 0 [Btu/lbm]; DELTApe_2_3 = 0 [Btu/lbm]

" Property/Function Calls:"

" DELTAh_2_3 = h[2] - h[3]

" h[3] = Enthalpy(WF\$,P=P[3],T=T[3]);

" s[3] = Entropy(WF\$,P=P[3],T=T[3]);

"

"

"Energy Balance, Thermal Expansion Valve {3 -> 4}"

Q_dot_tvx + W_dot_tvx*convert(W, Btu/hr) + m_dot * (DELTAh_3_4 + DELTAke_3_4 + DELTApe_3_4) = DELTAE_sys_tvx

" Assumptions:1) Steady State Operation; 2) No Work Interactions; 3) Adiabatic Device; "

" 4) Negligible Changes in Kinetic and Potential Energy."

" DELTAE_sys_tvx = 0 [Btu/hr]; W_dot_tvx = 0 [W]; Q_dot_tvx = 0 [Btu/hr];

" DELTAke_3_4 = 0 [Btu/lbm]; DELTApe_3_4 = 0 [Btu/lbm]

" Property/Function Calls:"

" DELTAh_3_4 = h[3] - h[4]

"

"

"Energy Balance, Evaporator {4 -> 1}"

Q_dot_evap + W_dot_evap*convert(W, Btu/hr) + m_dot * (DELTAh_4_1 + DELTAke_4_1 + DELTApe_4_1) =
DELTAE_sys_evap

" Assumptions:1) Steady State Operation; 2) No Work Interactions "

" 3) Negligible Changes in Kinetic and Potential Energy"

" DELTAE_sys_evap = 0 [Btu/hr]; W_dot_evap = 0 [W]

" DELTAke_4_1 = 0 [Btu/lbm]; DELTApe_4_1 = 0 [Btu/lbm]

" Property/Function Calls:"


```
" " DELTAh_4_1 = h[4] - h[1]
" " s[4] = Entropy(WF$,P=P[4],h=h[4]);
" " T[4] = Temperature(WF$,P=P[4],h=h[4])
" "
" "
"Overall System Performance Analysis:"
COP_R = Q_dot_evap / (W_dot_comp*convert(W, Btu/hr))
" "
" "
"System Error"
" " Error_Q = (Q_dot_evap - Q_data)/Q_data
" " Error_W = (W_dot_comp - W_data)/W_data
" " Error_eta = (eta_s-eta_data)/eta_data
```

APPENDIX II.

EES CODES FOR REFRIGERATION SYSTEM WITH TWO-PHASE FLUID INJECTION

File:Injection Model Verification_RG_12_7_2015.EES

3/19/2016 8:14:51 PM Page 1

EES Ver. 9.948: #0292: Mechanical Engineering - Marquette University

```
$UnitSystem ENG MASS DEG PSIA F
$TABSTOPS 0.5 1 1.5 2 2.5 in
```

"Rui Gu Creates The File On Decemler 6, 2015"

"Independent Variables Governing Refrigerant-Injected Vapor-Compression Cycle"

```
COP = COP ( r_p, Ratio_p, Ratio_m, x_inj ) "
" r_p = P[2] / P[1] "Overall Pressure Ratio"
" Ratio_p = (P_inj - P[1]) / (P[2] - P[1]) "Intermediate Pressure Ratio"
" Ratio_m = m_dot_inj / m_dot_total "Injection Mass Flow Rate Ratio"
" x_inj = x[8] "Injection Quality"
```

"Maximum Compressor Efficiency Case Verification"

m_dot_total = 670 [lbm/hr]; T_evap = 45 [F]; T_cond = 110 [F]; Ratio_m = 0.1; Ratio_p = 0.5

"The Refrigerant-Injected Vapor-Compression Cycle Model Verification"

Given Information:"

```
WF$ = 'R410a';
P[1] = Pressure(WF$, T=T_evap, x=1); T[1] = T_evap + 20 [F] "Compressor Inlet, 20 Degree Superheated"
P[2] = P[3]; "Compressor Outlet and Condenser Inlet"
P[3] = Pressure(WF$, T=T_cond, x=0); T[3] = T_cond - 15 [F] "Condenser Outlet, 15 Degree Subcooled"
P[4] = P[1]; "Evaporator Suction Pressure"
P[5] = P[6]; P[6] = P_inj; "Flash Tank"
P[7] = P[8]; "Internal Heat Exchanger"
P[8] = P_inj; P[9] = P_inj; "Compressor Injection Port Before Mixing"
P[10] = P_inj "Compressor Injection Port After Mixing"
```

"Locate Compressor Efficiency Based On Empirical Equation"

```
eta_1st = -1.46089 + 2.65662*r_p1 - 1.2226*r_p1^2 + 0.269856*r_p1^3 - 0.0293404*r_p1^4 + 0.001257*r_p1^5
r_p1 = P[9] / P[1] "First Stage Pressure Ratio"
eta_2nd = -1.46089 + 2.65662*r_p2 - 1.2226*r_p2^2 + 0.269856*r_p2^3 - 0.0293404*r_p2^4 + 0.001257*r_p2^5
r_p2 = P[2] / P[10] "Second Stage Pressure Ratio"
"
"
"
```

"Energy Balance, First Stage Compressor {1 -> 9}"

```
Q_dot_comp_1st + W_dot_comp_1st * convert(W, Btu/hr) + m_dot[1] * (DELTAh_1_9 + DELTAke_1_9 + DELTApe_1_9) =
DELTAE_sys_comp_1st
```

```
" Assumptions:1) Steady State Operation; 2) Adiabatic, Reversible Compression;"
" 3) Negligible Changes in Kinetic and Potential Energy; 4) Compressor Efficiency Based On Emprical Equation "
" DELTAE_sys_comp_1st = 0 [Btu/hr]; Q_dot_comp_1st = 0 [Btu/hr]
" DELTAke_1_9 = 0 [Btu/lbm]; DELTApe_1_9 = 0 [Btu/lbm]
" eta_1st = (h[1] - h_9s) / (h[1] - h[9])
" Property/Function Calls:"
" DELTAh_1_9 = h[1] - h[9]
" h[1] = Enthalpy(WF$,P=P[1],T=T[1])
" s[1] = Entropy(WF$,P=P[1],T=T[1])
" h_9s = Enthalpy(WF$,P=P[9],s=s[1])
" T[9] = Temperature(WF$,P=P[9],h=h[9])
" s[9] = Entropy(WF$,P=P[9],h=h[9])
```

" Mass Balance, First Stage Compressor {1 -> 9}"

```
" m_dot[1] = m_dot[9]
"
"
"
```

"Energy Balance, Injection Pt Mix {8,9-> 10}"

```
Q_dot_mix + W_dot_mix * convert(W, Btu/hr) + m_dot[8] * (DELTAh_8_10 + DELTAke_8_10 + DELTApe_8_10) + m_dot[9] *
(DELTAh_9_10 + DELTAke_9_10 + DELTApe_9_10) = DELTAE_sys_mix
```

```
" Assumptions:1) Steady State Operation; 2) Adiabatic, Reversible Compression;"
" 3) Negligible Changes in Kinetic and Potential Energy."
" DELTAE_sys_mix = 0 [Btu/hr]; W_dot_mix = 0 [W]; Q_dot_mix = 0 [Btu/hr]
" DELTAke_8_10 = 0 [Btu/lbm]; DELTApe_8_10 = 0 [Btu/lbm]"
```

```

" DELTAke_9_10 = 0 [Btu/lbm]; DELTApe_9_10 = 0 [Btu/lbm]
" Property/Function Calls:"
" DELTAh_8_10 = h[8] - h[10]
" DELTAh_9_10 = h[9] - h[10]
" h[8] = h_inj
" Mass Balance, Injection Pt Mix {8,9-> 10}"
" m_dot[8] + m_dot[9] = m_dot[10]
" m_dot[8] = m_dot_inj
"
"
"
"Energy Balance, Second Stage Compressor {10 -> 2}"
Q_dot_comp_2nd + W_dot_comp_2nd * convert(W, Btu/hr) + m_dot[10] * (DELTAh_10_2 + DELTAke_10_2 +
DELTApe_10_2) = DELTAE_sys_comp_2nd
" Assumptions:1) Steady State Operation; 2) Adiabatic, Reversible Compression;"
" 3) Negligible Changes in Kinetic and Potential Energy; 4) Compressor Efficiency Based On Empirical Equation"
" DELTAE_sys_comp_2nd = 0 [Btu/hr]; Q_dot_comp_2nd = 0 [Btu/hr]
" DELTAke_10_2 = 0 [Btu/lbm]; DELTApe_10_2 = 0 [Btu/lbm]
" eta_2nd = (h[10] - h_2s) / (h[10] - h[2])
" Property/Function Calls:"
" DELTAh_10_2 = h[10] - h[2]
" T[10] = Temperature(WF$,P=P[10],h=h[10])
" s[10] = Entropy(WF$,P=P[10],h=h[10])
" h_2s = Enthalpy(WF$,P=P[2],s=s[10])
" T[2] = Temperature(WF$,P=P[2],h=h[2])
" s[2] = Entropy(WF$,P=P[2],h=h[2])
" Mass Balance, Second Stage Compressor {10 -> 2}"
" m_dot[10] = m_dot[2]
" m_dot[2] = m_dot_total
"
"
"
"Energy Balance, Condenser {2 -> 3}"
Q_dot_cond + W_dot_cond * convert(W, Btu/hr) + m_dot[2] * (DELTAh_2_3 + DELTAke_2_3 + DELTApe_2_3) =
DELTAE_sys_cond
" Assumptions:1) Steady State Operation; 2) No Work Interactions;"
" 3) Negligible Changes in Kinetic and Potential Energy."
" DELTAE_sys_cond = 0 [Btu/hr]; W_dot_cond = 0 [W]
" DELTAke_2_3 = 0 [Btu/lbm]; DELTApe_2_3 = 0 [Btu/lbm]
" Property/Function Calls:"
" DELTAh_2_3 = h[2] - h[3]
" h[3] = Enthalpy(WF$,P=P[3],T=T[3])
" s[3] = Entropy(WF$,P=P[3],T=T[3])
" Mass Balance, Condenser {2 -> 3}"
" m_dot[2] = m_dot[3]
"
"
"
"Energy Balance, Thermal Expansion Valve 1 {3 -> 5}"
Q_dot_tvx_1 + W_dot_tvx_1 * convert(W, Btu/hr) + m_dot[3] * (DELTAh_3_5 + DELTAke_3_5 + DELTApe_3_5) =
DELTAE_sys_tvx_1
" Assumptions:1) Steady State Operation; 2) No Work Interactions; 3) Adiabatic Device;"
" 4) Negligible Changes in Kinetic and Potential Energy."
" DELTAE_sys_tvx_1 = 0 [Btu/hr]; W_dot_tvx_1 = 0 [W]; Q_dot_tvx_1 = 0 [Btu/hr]
" DELTAke_3_5 = 0 [Btu/lbm]; DELTApe_3_5 = 0 [Btu/lbm]
" Property/Function Calls:"
" DELTAh_3_5 = h[3] - h[5]
" T[5] = Temperature(WF$,P=P[5],h=h[5])
" s[5] = Entropy(WF$,P=P[5],h=h[5])
" x[5] = Quality(WF$,P=P[5],h=h[5])
" Mass Balance, Thermal Expansion Valve 1 {3 -> 5}"
" m_dot[3] = m_dot[5]
"
"

```

```

"
"
"Energy Balance, Flash Tank {5 -> 6,7}"
Q_dot_FT + W_dot_FT * convert(W, Btu/hr) + m_dot[6] * (DELTAh_5_6 + DELTAke_5_6 + DELTApe_5_6) + m_dot[7] * (
DELTAh_5_7 + DELTAke_5_7 + DELTApe_5_7) = DELTAE_sys_FT
" Assumptions:1) Steady State Operation; 2) Adiabatic, Reversible Compression;"
" 3) Negligible Changes in Kinetic and Potential Energy."
" DELTAE_sys_FT = 0 [Btu/hr]; W_dot_FT = 0 [W]; Q_dot_FT = 0 [Btu/hr]
" DELTAke_5_6 = 0 [Btu/lbm]; DELTApe_5_6 = 0 [Btu/lbm]
" DELTAke_5_7 = 0 [Btu/lbm]; DELTApe_5_7 = 0 [Btu/lbm]
" Property/Function Calls:"
" DELTAh_5_6 = h[5] - h[6]
" DELTAh_5_7 = h[5] - h[7]
" DELTAh_5_6 - DELTAh_5_7 = 0
" {h[6] = Enthalpy(WF$,P=P[6],x=0)}
" {h[7] = Enthalpy(WF$,P=P[7],x=1)}
" Mass Balance, Flash Tank {5 -> 6,7}"
" m_dot[5] = m_dot[6] + m_dot[7]"
" Ratio_m = m_dot[7] / m_dot[5]"
"
"
"Energy Balance, Internal Heat Exchanger {7 -> 8}"
Q_dot_IHX + W_dot_IHX * convert(W, Btu/hr) + m_dot[7] * (DELTAh_7_8 + DELTAke_7_8 + DELTApe_7_8) =
DELTAE_sys_IHX
" Assumptions:1) Steady State Operation; 2) No Work Interactions "
" 3) Negligible Changes in Kinetic and Potential Energy"
" DELTAE_sys_IHX = 0 [Btu/hr]; W_dot_IHX = 0 [W]; "Assuming "Q_dot_IHX =0 [Btu/hr]
" DELTAke_7_8 = 0 [Btu/lbm]; DELTApe_7_8 = 0 [Btu/lbm]
" Property/Function Calls:"
" DELTAh_7_8 = h[7] - h[8]
" T[7] = Temperature(WF$,P=P[7],h=h[7])
" s[7] = Entropy(WF$,P=P[7],h=h[7])
" T[8] = Temperature(WF$,P=P[8],h=h[8])
" s[8] = Entropy(WF$,P=P[8],h=h[8])
" x[8] = Quality(WF$,P=P[8],h=h[8])
" Mass Balance, Internal Heat Exchanger {7 -> 8}"
" m_dot[7] = m_dot[8]"
"
"
"Energy Balance, Thermal Expansion Valve 2 {6 -> 4}"
Q_dot_tv_2 + W_dot_tv_2 * convert(W, Btu/hr) + m_dot[6] * (DELTAh_6_4 + DELTAke_6_4 + DELTApe_6_4) =
DELTAE_sys_tv_2
" Assumptions:1) Steady State Operation; 2) No Work Interactions; 3) Adiabatic Device; "
" 4) Negligible Changes in Kinetic and Potential Energy."
" DELTAE_sys_tv_2 = 0 [Btu/hr]; W_dot_tv_2 = 0 [W]; Q_dot_tv_2 = 0 [Btu/hr]
" DELTAke_6_4 = 0 [Btu/lbm]; DELTApe_6_4 = 0 [Btu/lbm]
" Property/Function Calls:"
" DELTAh_6_4 = h[6] - h[4]
" T[6] = Temperature(WF$,P=P[6],h=h[6])
" s[6] = Entropy(WF$,P=P[6],h=h[6])
" Mass Balance, Thermal Expansion Valve 2 {6 -> 4}"
" m_dot[6] = m_dot[4]"
"
"
"Energy Balance, Evaporator {4 -> 1}"
Q_dot_evap + W_dot_evap * convert(W, Btu/hr) + m_dot[4] * (DELTAh_4_1 + DELTAke_4_1 + DELTApe_4_1) =
DELTAE_sys_evap
" Assumptions:1) Steady State Operation; 2) No Work Interactions "
" 3) Negligible Changes in Kinetic and Potential Energy"
" DELTAE_sys_evap = 0 [Btu/hr]; W_dot_evap = 0 [W]
" DELTAke_4_1 = 0 [Btu/lbm]; DELTApe_4_1 = 0 [Btu/lbm]
" Property/Function Calls:"
" DELTAh_4_1 = h[4] - h[1]"

```

```
"      " s[4] = Entropy(WF$,P=P[4],h=h[4])
"      " T[4] = Temperature(WF$,P=P[4],h=h[4])
"      Mass Balance, Compressor {4 -> 1}
"      " m_dot[4] = m_dot[1]
"      "
"      "
"      "
"Overall System Performance Analysis:"
"      "COP_R = Q_dot_evap / ((W_dot_comp_1st + W_dot_comp_2nd) * convert(W, Btu/hr))
"      "eta_inj = (m_dot[1] * (h[1] - h_9s) + m_dot[2] * (h[10] - h_2s)) / (m_dot[1] * (h[1] - h[9]) + m_dot[2] * (h[10] - h[2]))
```